

AD-A117 373

NAVAL OCEAN SYSTEMS CENTER SAN DIEGO CA  
LMDS LIGHTWEIGHT MODULAR DISPLAY SYSTEM.(U)  
FEB 82 A D GOMEZ, S W WOLFE, E W DAVENPORT  
NOSC/TR-767

F/6 9/2

UNCLASSIFIED

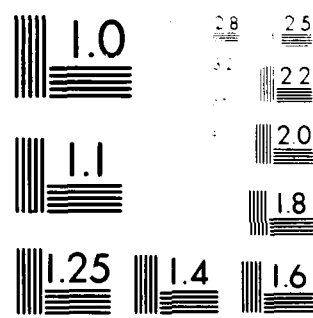
NL

1 of 1  
AD-A  
117373

NOSC



END  
DATE  
FILMED  
08:82  
DTIC



U.S. GOVERNMENT PRINTING OFFICE  
1964 O - 348-100

12  
**NOSC**

NOSC TR 767

AD A117373

NOSC TR 767

Technical Report 767

# **LMDS LIGHTWEIGHT MODULAR DISPLAY SYSTEM**

AD Gomez  
SW Wolfe  
EW Davenport  
BD Calder

16 February 1982

DTC FILE COPY

**DTIC**  
**ELECTE**  
JUL 22 1982  
**S** **D**

Approved for public release; distribution unlimited.

**F**

**NAVAL OCEAN SYSTEMS CENTER  
SAN DIEGO, CALIFORNIA 92152**

82 07 22 007



NAVAL OCEAN SYSTEMS CENTER, SAN DIEGO, CA 92152

---

AN ACTIVITY OF THE NAVAL MATERIAL COMMAND

SL GUILLE, CAPT, USN

Commander

HL BLOOD

Technical Director

ADMINISTRATIVE INFORMATION

The work in this document was sponsored by NAVSEA 61R under project F21202, subproject SF21202491/20419, work unit 824-CC55. This report covers work from October 1977 to January 1982 and was approved for publication on 16 February 1982.

Released by  
RC Kolb, Head  
Tactical Command and Control Division

Under authority of  
JH Maynard, Head  
Command Control - Electronic  
Warfare Systems and  
Technology Department

UNCLASSIFIED

SECURITY CLASSIFICATION OF THIS PAGE (When Data Entered)

REPORT DOCUMENTATION PAGE		READ INSTRUCTIONS BEFORE COMPLETING FORM
1. REPORT NUMBER NOSC Technical Report 767 (TR 767)	2. GOVT ACCESSION NO. AD-A117373	3. RECIPIENT'S CATALOG NUMBER
4. TITLE (and Subtitle) LMDS LIGHTWEIGHT MODULAR DISPLAY SYSTEM		5. TYPE OF REPORT & PERIOD COVERED Oct 77 to Jan 82
7. AUTHOR(s) AD Gomez      EW Davenport SW Wolfe      BD Calder		6. PERFORMING ORG. REPORT NUMBER
9. PERFORMING ORGANIZATION NAME AND ADDRESS Naval Ocean Systems Center San Diego, CA 92152		8. CONTRACT OR GRANT NUMBER(s)
11. CONTROLLING OFFICE NAME AND ADDRESS Naval Sea Systems Command Washington, DC 20362		10. PROGRAM ELEMENT, PROJECT, TASK AREA & WORK UNIT NUMBERS F21202 SF21202491/20419 824-CC55
14. MONITORING AGENCY NAME & ADDRESS (if different from Controlling Office)		12. REPORT DATE 16 February 1982
		13. NUMBER OF PAGES 90
		15. SECURITY CLASS. (of this report) UNCLASSIFIED
		15a. DECLASSIFICATION/DOWNGRADING SCHEDULE
16. DISTRIBUTION STATEMENT (of this Report)  Approved for public release; distribution unlimited.		
17. DISTRIBUTION STATEMENT (of the abstract entered in Block 20, if different from Report)		
18. SUPPLEMENTARY NOTES		
19. KEY WORDS (Continue on reverse side if necessary and identify by block number)		
Distributed Processing      Power Distribution      Modular Display      Low Cost Tactical Display      Tactical Tablet      Lightweight Display      General Purpose Display Functional Modules      Touch Entry      Imbedded Processors Symbol Generator      Display, TV      Video Distribution Vector Generator      High Resolution TV      Low Power Display		
20. ABSTRACT (Continue on reverse side if necessary and identify by block number)		
<p>The Lightweight Modular Display System (LMDS) consists of a set of low-cost modules integrated into a low-power, lightweight, general-purpose display system. LMDS was developed for broad application aboard surface combatant command and control systems and noncombatant platforms in the 1990 time frame.</p> <p>The LMDS introduces innovative approaches to human interface, thermal and shock management, power distribution, architecture, sensor display, and system management. This design approach enables the LMDS to significantly improve upon operator efficiency, cost, size, weight, and maintenance factors as compared to traditional display systems.</p>		

DD FORM 1473

JAN 79

EDITION OF 1 NOV 65 IS OBSOLETE

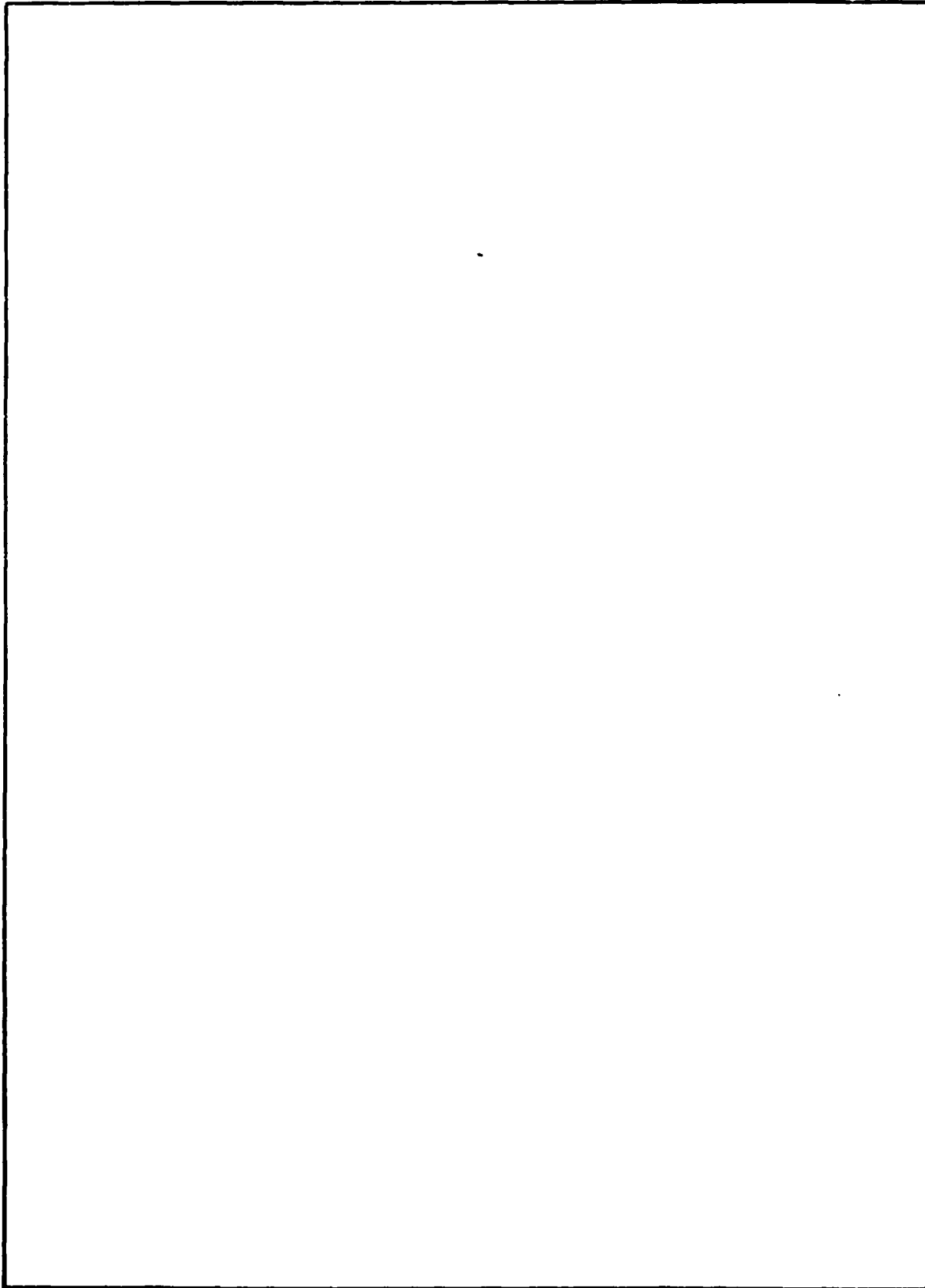
S/N 0102-LF-014-6601

UNCLASSIFIED

SECURITY CLASSIFICATION OF THIS PAGE (When Data Entered)

UNCLASSIFIED

SECURITY CLASSIFICATION OF THIS PAGE (When Data Entered)



S/N 0102- LF- 014- 6601

UNCLASSIFIED

SECURITY CLASSIFICATION OF THIS PAGE(When Data Entered)

## CONTENTS

### Section

1	INTRODUCTION . . .	page 1-1
	General Description . . .	1-1
	System Requirements . . .	1-1
	System Objectives . . .	1-3
	Combat Effectiveness . . .	1-3
	Life Cycle Cost Advantages . . .	1-3
2	DESIGN APPROACH . . .	2-1
	Purpose . . .	2-1
	Man-machine Interface . . .	2-2
	Tablet-man Interface . . .	2-2
	Display-man Interface . . .	2-2
	Console Architecture . . .	2-3
	Electrical Considerations . . .	2-3
	Console Modularity . . .	2-3
	Scan Converter . . .	2-3
	Map Generator . . .	2-3
	Power System . . .	2-4
	Digital Raster Television Standard (DIRTS) Code Design . . .	2-4
	Interfaces and Interconnection . . .	2-5
	Built-in Test Equipment (BITE) . . .	2-6
	Mechanical Considerations . . .	2-7
	Module Goals . . .	2-7
	Module Heat Sink . . .	2-7
	Module Chassis . . .	2-8
	Module Panel . . .	2-8
	Support Frame Design Goals . . .	2-8
	Module/Frame Interface . . .	2-9
	Vibration Testing . . .	2-10

## CONTENTS (Continued)

### Section

	Thermal Approach . . .	2-11
	Maintenance Philosophy . . .	2-12
3	PROTOTYPE SYSTEM FUNCTION . . .	3-1
	Module Functional Characteristics . . .	3-1
	Display Module . . .	3-1
	Tablet Module . . .	3-4
	Intercom Unit . . .	3-5
	Scan Converter . . .	3-6
	Interface/Processor Module . . .	3-8
	Vector Generator Module . . .	3-8
	Character Generator Module . . .	3-9
	Map Generator Module . . .	3-11
	Power Supply Module . . .	3-12
	Unattended Equipment Modules . . .	3-14
	Scan Converter . . .	3-14
	Map Generator . . .	3-14
	Digital Sync Generator DIRTS Code . . .	3-16
	Junction Box/Converter . . .	3-16
	Future Modules . . .	3-16
	Color Display . . .	3-16
	Keyboards . . .	3-17
	Slow Scan Display Transmitter . . .	3-17
	Unattended Equipment . . .	3-18
	Radar Recorder . . .	3-18
	Digital Bus Recorder . . .	3-18
	Video Sensor Simulation . . .	3-18
	Sensor Switchboard . . .	3-18
	System Configuration and Specifications . . .	3-18
	System Operation . . .	3-22



## CONTENTS (Continued)

### Section

#### 4 APPENDICES

- Appendix A - Tablet vs. Trackball Comparative Test Data . . . A-1
- Appendix B - LMDS Module Assembly Thermal Design Summary . . . B-1
- Appendix C - LMDS Shock and Vibration Test Data . . . C-1

### ILLUSTRATIONS

- 1-1 Lightweight modular display system . . . page 1-2
- 2-1 LMDS approach to meeting Fleet needs . . . 2-1
- 2-2 LMDS modular design approach . . . 2-4
- 3-1 LMDS console module configuration . . . 3-1
- 3-2 LMDS functional module block diagram . . . 3-2
- 3-3 LMDS display module . . . 3-2
- 3-4 LMDS display functional block diagram . . . 3-3
- 3-5 Functional block diagram of LMDS entry tablet . . . 3-4
- 3-6 Operator using LMDS digitizer tablet . . . 3-6
- 3-7 LMDS interface unit functional block diagram . . . 3-9
- 3-8 LMDS map generator block diagram . . . 3-12
- 3-9 LMDS power supply functional block diagram . . . 3-13
- 3-10 LMDS scan converter broadcaster . . . 3-15

### TABLES

- 2-1 Predicted vs. measured fundamental frequencies . . . page 2-10
- 2-2 Reanalyzed vs. measured fundamental frequencies . . . 2-10

## SECTION 1

### INTRODUCTION

#### GENERAL DESCRIPTION

The Lightweight Modular Display System (LMDS) consists of a set of low-cost modules integrated into a low-power, lightweight, general-purpose display system (fig 1-1). LMDS was developed for broad application aboard surface combatant command and control systems and noncombatant platforms in the 1990 time frame.

The LMDS introduces innovative approaches to human interface, thermal and shock management, power distribution, architecture, sensor display, and system management. This design approach enables the LMDS to significantly improve upon operator efficiency, cost, size, weight, and maintenance factors as compared to traditional display systems.

#### SYSTEM REQUIREMENTS

The major requirement is to provide an inexpensive suite of display modules which exhibit minimum weight, volume, and power consumption without sacrificing high reliability/maintainability and man-machine interface performance. The optimization of the man-machine interface is crucial to applications requiring minimum manning levels.

With the technical evaluation of display modules, it is imperative that allowances be made for graceful integration of new requirements and system upgrades. Primary design consideration has been given to thermal and mechanical packaging to minimize the redundant weight/strength tradeoff typical of conventional military structures.

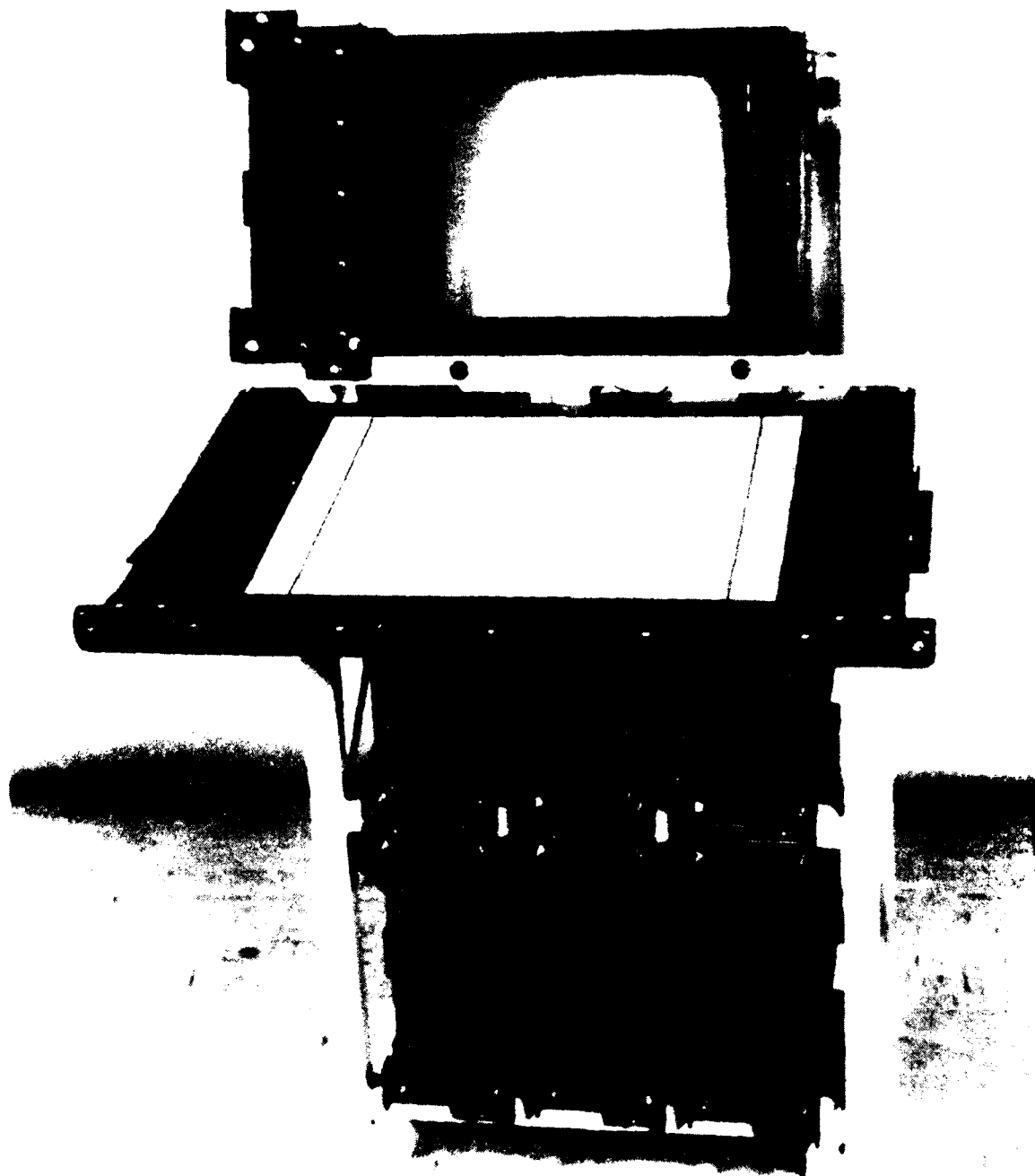


Figure 1-1. Lightweight Modular Display System.

## SYSTEM OBJECTIVES

### Combat Effectiveness

Combat effectiveness represents the relationship between cost, in terms of the quantity of something available, its availability or uptime, and the efficiency with which it executes its function. In this context, LMDS design goals are to lower the system cost so that more consoles can be procured, to increase the reliability of the system so that the availability of the system is greater, to reduce the time for fault location and to do this with a new man-machine interface. This new interface will permit a more efficient operator sequence that integrates sensor and information displays coordinated to reduce the operator's response time. To achieve these objectives, a considerable departure from existing architecture, packaging, man-machine interface, and appearance is necessary.

A system's cost effectiveness takes many forms; for LMDS, it is the ability to meet a variety of display requirements based on standard functions. This means that the cost to produce a particular display function can be met in the most economical fashion and at the same time provide for later upgrades. By increasing the utilization of particular functions, overall function costs can be reduced. This, in turn, enhances combat effectiveness by allowing more equipment to be placed on more ships.

### Life Cycle Cost Advantages

The module nature of LMDS is the principal term in the life cycle cost advantage equation. The modular approach avoids the problem of system obsolescence before wear-out. In the past, the cost of replacing the system often precluded substitution of a better system. The modular nature of LMDS provides a mechanism for graceful upgrade of a unit to meet new threats or changing mission requirements. This procedure for procurement of the functional module allows for the most cost-effective upgrades possible.

Another life cycle cost advantage for LMDS is the fact that functional modules are able to absorb technological change. Many of the components

necessary to produce equipment designed today are no longer available in tomorrow's marketplace. By adopting functional modules, there is enough system flexibility to permit less expensive implementations of today's functions to be added in the near future. Therefore, as procurements of spares continue in the face of technological change, there is little impact on the deployment of either old or new systems. In short, the LMDS modules become technology-transparent while maintaining the lowest possible sparing cost for the system.

Accession For	
MTIS GRA&I	<input checked="checked" type="checkbox"/>
DTIC TAB	<input type="checkbox"/>
Unannounced	<input type="checkbox"/>
Justification	
By	
Distribution/	
Availability Codes	
Dist	Avail and/or Special
A	



## SECTION 2

### DESIGN APPROACH

The LMDS has been designed to meet the operational display requirements of the Fleet within reasonable cost constraints. The LMDS must be easy to install, simple to operate, and must demonstrate reliability plus the ability to be easily maintained and upgraded. These design goals have been manifested in a lightweight, low power, low cost prototype which has achieved a modular, platform configuration service by convection cooling. Figure 2-1 demonstrates how system goals have been integrated with design philosophy.

Technical Approach	Fleet Needs					
	Low Cost	Simple Installation	Simple To Operate	Reliable	Easy To Maintain	Easily Upgraded
Large circuit boards	✓			✓	✓	✓
High component count	✓			✓	✓	
High chip complexity	✓			✓		
Low power				✓		
Low junction temp				✓		
Convection cooled	✓	✓		✓	✓	✓
Low connector count	✓			✓	✓	✓
Minimal cables	✓	✓		✓	✓	
Lightweight modules	✓	✓			✓	
Configuration specific modules		✓	✓		✓	✓

Figure 2-1. LMDS approach to meeting Fleet needs.

## MAN-MACHINE INTERFACE

### Tablet-man Interface

The LMDS design approach emphasizes reduction of the number of displays and the different entry devices that are typically used in display devices. The approach utilizes a single pressure sensitive surface or digitizer tablet for data entry and a single display for operator feedback. A few fixed function buttons may be required to augment this simple approach. The advantage of this approach is in the programmable control surface that can be redefined with either software or firmware. It is intended that the CRT provide the labels and menus for the different controls. For the entry of alphanumeric data, the tablet surface may be defined by printed overlay. This allows the same area of the tablet to be used for different functions at different times. This minimizes the amount of control panel required and makes the console surface smaller, lighter, and less costly.

All of these approaches are sufficiently different; a commercial display generator, its controller, and a pressure sensitive surface have been used to test the control techniques to find out if the results are effective. This image prototype test unit can be expanded to test the raster scan symbols, resolution, and label techniques that are required. Later, the display can be upgraded to test the sum of all the control, graphics, and radar images operating together.

### Display-man Interface

The LMDS represents a departure from typical display console man-machine interfaces. Its approach eliminates virtually all of the manual controls that are traditionally used on a console. The design replaces standard controls with a pressure-sensitive tablet responding to finger or stylus.

This conversion was effected for several reasons. Buttons and switches can, for example, be a liability in an environment where there is frequent liquid spillage; they require back panel illumination which consumes additional electrical power; they need a considerable amount of circuitry to interface

their buttons up to control word level; and they occupy panel space which results in increased footprint for the equipment.

The trackball is the most precise instrument a display console operator can use to position a cursor. This precision is insufficiently compelling, however, to overshadow the overall advantage of the pressure-sensitive tablet. Appendix A outlines an experiment which was performed to compare the relative accuracies of trackball and tablet. For all practical purposes, and to the precision needed for LMDS, the tablet meets the tracking requirements. It creates distinct advantages in terms of tracking response time because it processes in an absolute X-Y reference. A system advantage is gained in the reduced complexity of circuitry needed to support these functions.

## CONSOLE ARCHITECTURE

### Electrical Considerations

Console Modularity. The preliminary LMDS architecture consists of a high resolution (1075-line) TV based display console with a single display element. The success of this architecture depends heavily upon the principle of functional modularity expressed in figure 2-2. The modules in this design are considered individual peripherals to an internal interface processor. This configuration allows for future modifications and upgrades which make the individual module functions independent of both manufacturer and technology.

Scan Converter - The LMDS design requires a scan converted image for any sensor input to the console. By standardizing the interface to the display console, a more versatile system is created which easily processes new information appearing in a uniform data format. This system architecture employs a multiuser configuration that results in cost savings.

Map Generator - The LMDS is able to store worldwide maps and charts on line in computer mass memory and is able to rapidly recall and display them.



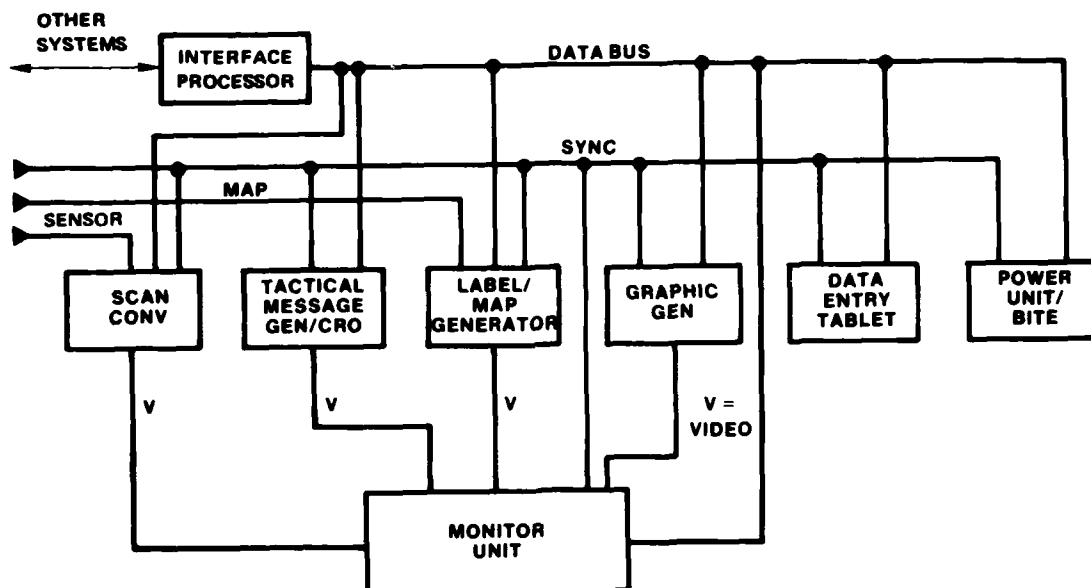


Figure 2-2. LMDS modular design approach.

This project has developed a low-cost, efficient TV monitor display by reorganizing map data stored as a series of compressed horizontal lines. The map is then equivalent to a series of on and off elements along a line of latitude.

Power System - Power to the console has been limited to 250 W. Power reduction has been achieved by minimizing interface and data exchange. Specific techniques for accomplishing additional reductions include use of switching power supplies to increase efficiency of power distribution and dynamic power turn-off methods that remove power from functions not being used.

Digital Raster Television Standard (DIRTS) Code Design - Early in the design phase of LMDS it became apparent that standard television synchronization techniques were inadequate. They were not able to synchronize the different video outputs from the various modules to produce a jitter-free and accurate overlay. The principal reason for this is that the rise time of the standard synchronization is not fast enough to accurately position a pel - 1 pel has a duration of only 18 nanoseconds.

To provide an accurate timing edge for all of the display modules, it was necessary to generate a new synchronization with very fast rise time. Since typical synchronization separators are analog devices producing drift and jitter, it was advantageous to avoid that approach and, instead, achieve an all digital design for the synchronization structure. The resulting synchronization was based on having small code words Manchester encoded in a continuous carrier which could be used to localize the timing points necessary to generate a standard television synchronization waveform. Examples are a 4-bit code placed at the beginning of horizontal synchronization; another 4-bit code placed at the end of horizontal synchronization; and a code at the beginning of front porch, etc.

In addition to the standard television fiducial points, others have been added which assist the various modules in doing their particular jobs. This technique has been expanded to include numbering every line of the image in both the even and odd fields. This way the various display modules do not have to generate their own line counters, hence, it results in a more accurate and assured image timing. The entire synchronization structure is placed on a carrier which is one quarter of the pel frequency. Circuitry has been designed which regenerates pel clock from this one-quarter pel clock rate.

Interfaces and Interconnection - The power-saving feature of minimum cabling and interfaces is enhanced by lower weight, lower cost, and increased reliability. Implementation of this concept is facilitated by the modular design approach of LMDS.

To appreciate the LMDS interface design, it is important to understand some primary functional objectives of the system. One of the desirable characteristics of the LMDS bus structure includes a network capable of supporting large and extensive modifications to the number of modules, while leaving existing module software intact. This feature requires a common word format sufficiently flexible to allow a variety of communications to occur without traffic problems. To achieve this objective, it is important to have messages sent with source, destination, and type addresses. The intention is to have a

feedback system to perform diagnostics that can identify message users regardless of message type. To prevent obvious recurrent collisions with multiple users, a time-out scheme was used.

Since all of the foregoing functions are nearly met by the ETHERNET bus structure and since the chips for this scheme are being designed, it is advantageous for LMDS to use this protocol. This will allow LMDS to network with the commercial equipment that will be produced to this new de facto standard and shore site equipment installations to use many commercial systems without the high cost of special interfaces and translators.

The use of this ETHERNET design does not mean that the NTDS interface would be eliminated. What is anticipated is the use of ETHERNET at a low level of system interface, ie internal to the console intermodule. This low level bus would interface to the higher level through a portal defined as an interface/processor unit. The function of the interface unit is to reformat and screen data for the modules that form a LMDS console or display system.

Built-In Test Equipment (BITE) - The LMDS design uses layered built-in test equipment (BITE). The first layer of BITE is located within the module itself and performs two separate functions. The first function is a built-in self-diagnostic for the processor within the module. The second function internal to the module is one that supports external test equipment for individual module testing. At this layer, each unit has an internal RS-232 port which allows external test programs to be down loaded to the unit for special diagnostic testing.

The second layer of BITE operates from a system perspective and is performed by a built-in test processor contained within the power supply module. To support this processor's function, both ends of the ETHERNET bus are terminated at the power supply. This permits the built-in test processor to look at cable continuity as well as message traffic on the bus. The built-in test is intended to support a maintenance philosophy which is based on three levels of maintenance.

The first level of maintenance is module replacement. The second level involves board isolation within a module, and the third level is component replacement on the boards.

#### Mechanical Considerations

The LMDS tactical console configuration consists of an open framework with space for six electronic modular packages beneath a desk-top high shelf. Above the shelf is a communications module and a CRT display.

The system is intended to serve as a general purpose data entry and display console. It is constructed as a lightweight, low-power, easily maintainable system able to withstand Navy shipboard environments. The following paragraphs will discuss LMDS mechanical design as it relates to module goals, support frame design goals, vibration testing, and thermal testing.

Module Goals - The module design started with electronic requirements for two large circuit boards or tiled boards equal to two 10 inch by 15 inch cards having a maximum power of 25 W. Natural convection cooling was selected as the primary cooling mode for the module. A standard finned aluminum extrusion was selected for the heat sink - the preliminary mechanical package was designed around this extrusion. Package requirements provide a simple functional enclosure of 5 inches wide by 12 inches high by 18 inches deep and a weight limit of 25 pounds. The package must be maintainable and repairable with electrical connectors mounted through the heat sink going directly to the circuit board. The front panel protects exposed components from a console operator's feet. The module structure is a part of the support frame structure where feasible.

Module Heat Sink - The module heat sink is a standard 6063-T5 finned aluminum extrusion available from several fabricators. Initial module size was selected as 5.0 inches wide by 11.4 inches high by 16.5 inches deep. The extrusion is machined on the fin side to provide connector mounting surfaces and frame structure clearance. The module interior surface is designed to receive 16 or more press studs with 1/2 inch diameter threaded aluminum spacers screwed to them. The circuit boards fit over the studs with the

spacers in contact with the board and heat sink to provide a conduction heat transfer path from the board to the base of the heat sink. The press studs can be easily added, removed, or relocated to satisfy any circuit board/component configuration within the 10 by 15 inch area. An EMI gasket groove is machined in the heat sink to provide electrical radiation protection and drip proofing. A minimum heat sink base thickness of 0.125 inch was selected to reduce conduction heat transfer thermal resistance and minimize temperature gradients. Multiple machine screws are used to assure heat sink/chassis interface register and EMI-RFI seal.

Module Chassis - The chassis is a thin walled aluminum alloy frame with open sides and front. It is designed to permit easy removal of either heat sink assembly. The rear of the chassis contains an unsealed shear pin receptacle. When installed in the frame, the receptacle is mated with a close fitting pin which maintains EMI and drip-proof integrity.

Module Panel - The panel is machined from a standard aluminum alloy channel extrusion. It is designed to act as a shear panel for the front of the lower frame. Each panel is pinned in four places to the frame with close fitting pins. An EMI gasket groove is also machined in the panel for shielding. The panel has screw holes to secure it to each heat sink and the chassis. Two multiple lead captive thumb screws are provided in the panel assembly to secure the module to the frame. The channel flanges are used to guard the panel mounted components. The flange ears act as protection for knobs and controls, and the cut out flange sections provide connector access.

Support Frame Design Goals - The console frame supports the display system electronics. The tube frame supports up to seven modules, a display unit, and an electronic tablet. The open frame permits free air movement over the natural convection cooled system. The design goal was 23 inches wide by 18 inches deep by a 30-inch high writing surface and an inclined display frame support. Target console weight was 250 pounds. The frame was required to be separate for ease of installation and passage through hatches. A minimum natural frequency of 50 Hz was selected for all members and components in the console. This vibration goal is consistent with the new, small, high-speed Navy ships being constructed. Console dimensions were kept to a minimum

to reduce frame weight. Console size is 21.5 inches wide at the base, 26.0 inches wide at the writing surface, and 48.0 inches in overall height. The depth is 17.9 inches at the base with the module panel flanges extending 1 inch toward the operator. The shelf height is 29.5 inches and the display screen mounting is tilted upward 15 degrees. The viewing screen within the display is tilted upward an additional 10 degrees for operator viewing and to lower the center of gravity of the display module.

The lower frame is designed to contain six electronic modules. It consists of 1.25 and 1.0 inch square, 0.125-inch wall aluminum tubing. Four vertical corner posts support the upper frame. The lower diagonals are 1.25-inch square tubes with 1.0-inch square tubes inside to support shock loads when inclined 30 degrees. Mounting angles at the base were found deficient during vibration tests and have been revised to square tubing and corner blocks. The top corners have insert blocks for top frame attachment. The frame back has an "X" member and the module panels are each pinned (four places) to the front of the frame with adjustable eccentric shear pins. The modules are supported at the rear of the frame with adjustable shear pins. A dummy panel should be used for structural integrity when a module is not required.

The upper frame is designed to support the console display unit, one module, and the digitizer shelf, and is intended to be separable from the bottom frame for hatch entry. It is attached to the lower frame with expandable bolts that can create an intimate joint and which are used to take both shear and tension loads.

Module/Frame Interface - The modules are secured to the frame with two captive locking screws in the panel and floating receptacles in the frame. The screws retain the modules in the frame and provide quick access for repairs. Each module rests on a thin, teflon-coated, sheet metal angle which acts as a slide during module installation into the frame. Five adjustable pins must be fitted for each module during installation. The module location is interchangeable but only after shear pin adjustment with a minimum of tools.

Vibration Testing - The LMDS framework is designed to meet the shipboard vibration requirements of MIL-STD-167-1. Comparative vibration tests were performed on the LMDS fabricated framework and on a computer-simulated analytical model. The results of the comparison are discussed in the following paragraphs. A detailed description of actual test methods is contained in Appendix C.

Table 2-1 compares the fundamental frequencies for the analytical and test results.

Table 2-1. Predicted vs. measured fundamental frequencies.

	Analytical Frequencies (Hz)	Test Frequencies (Hz)
Fore-to-aft	86	30
Side-to-side	91	45
Vertical	<100	68

Clearly, the results do not compare very well. After comparing the analytical model with the test results, some obvious differences were noted. The first difference was in the way the structure was fastened to the deck. In the analytical model, the structure was assumed to be welded to the deck. In the actual tests, the structure was clamped to the vibration table with three clamps along each of the 1-1/4 x 1-1/4 x 1/4 equal leg angles. There was one clamp at the middle of each angle and one 2 inches from each end. The two angles and twelve 3/8 x 1 3/4-inch steel bolts had much more flexibility than if the four legs were welded to the table. The analytical model was changed to simulate the clamping. The results are shown in table 2-2.

Table 2-2. Reanalyzed vs. measured fundamental frequencies.

	Clamped Base Analytical Frequencies (Hz)	Test Frequencies (Hz)
Fore-to aft	30	30
Side-to-side	44	45
Vertical	77	68

It is obvious from the above results that the method of fastening the structure base to the deck makes a large difference in the fundamental modes of vibration. The best method of attachment would be to weld the structure to the deck. Next best would be to weld the base to a thick plate and bolt the plate to the deck. A third option would be to weld a special corner block to each leg that can be bolted to the floor - this approach has been selected.

Another difference between the analytical model and tested structure is the way the dummy load was attached to the CRT. In the analytical model, the load was distributed among the CRT grid points. In the tested structure, an 8 pound steel plate was bolted with four 1/4 inch steel bolts to an 8 pound aluminum plate. Two of these were made, with one bolted to the rear of the CRT and one bolted at the front. All of these bolts behave like stiff springs with the attached masses able to move in all three directions when under vibration.

A third noticeable difference was in the first natural frequency of the shelf. The analytical model showed a resonance at 57 Hz. The real structure showed a shelf resonance at 95 Hz. This difference can be accounted for in the way the shelf structure was welded together. The structural triangle on each side of the shelf turned out to be somewhat smaller than the analytical model due to the cross-sectional size of the square tube. This is the reason the frequency of resonance is somewhat higher.

Future test requirements include vibrating the structure to MIL-STD-167-1 and shocking to MIL-S-901C. The modifications for the base mounting have been redesigned to more firmly attach the four legs to the deck or test-bed.

Future testing will be delayed until more accurate weights and the actual electronic hardware have been installed. This will make the tests more valid and should increase the fundamental frequencies since the actual weights and distributions are expected to be smaller than the dummy weights.

Thermal Approach - The primary goal of effective thermal design is to control electronic part temperatures within specific limits that are consistent with electronic performance, reliability requirements, and system design



goals. The magnitude of the heat dissipation and resulting part temperatures can vary over a wide range for a specific cooling technique, depending on the design of a particular system. Frequently, more than one method can be used for different applications. The final system selection eventually depends on a tradeoff between cooling system design requirements, system design considerations, and life cycle costs.

A preliminary steady-state thermal analysis was performed on the conceptual LMDS system design to determine if the configuration could meet thermal design requirements. The proposed design utilized natural convection as the primary cooling mode for console electronics. Other cooling techniques such as forced air, liquid, or heat pipes would be considered if natural convection could not meet the system thermal design requirements under worst case operating conditions. This is a departure from conventional designs that normally require more complex and less reliable fans or heat exchanger systems to provide temperature control. Natural convection offers the most simple, reliable, and least costly system. Other parameters considered in the selection and design of a cooling system included part temperature limits, environmental conditions, reliability, weight, space, and life cycle costs.

The thermal analysis was based upon natural convection cooling and estimated heat loads. The results of this analysis indicate that a natural convection cooled design concept is feasible if sufficient space is available for heat dissipating surfaces and adequate internal heat conduction paths can be maintained. A more detailed discussion of LMDS thermal test results is contained in Appendix B.

#### **MAINTENANCE PHILOSOPHY**

The overall LMDS maintenance approach is divided into three levels of increasing complexity. The first level of maintenance may be performed on-site where a faulty module is simply removed and replaced. Second tier maintenance consists of board-level repair which may be conducted at an on-site intermediate repair facility. Finally, depot-level maintenance requires that a faulty unit be removed to a remote repair site for extensive overhaul.

LMDS fault isolation is intended to be sufficiently simple so that first echelon maintenance can be performed by the operator. To achieve this objective, the data interfaces between module and display unit are kept as uncomplicated as possible. With specific topics as video coming from each box, the operator can determine the origin of a fault by determining which video is faulty.

## SECTION 3

### PROTOTYPE SYSTEM FUNCTION

#### MODULE FUNCTIONAL CHARACTERISTICS

The full LMDS module configuration consists of the monitor unit, data entry tablet, intercom unit, scan converter, interface/processor, vector generator, character generator, map generator, and power supply. The relationship of console modules is expressed in figure 3-1. The basic operational design integrated into LMDS modules is represented in figure 3-2.

#### Display Module

The display module currently being designed for LMDS is a 15-inch diagonal raster display which operates from the internal system ETHERNET bus, the DIRTS (Digital Raster Television Standard) decoder bus, and inputs from each of the modules capable of generating video. The display unit is pictured in figure 3-3. The total power consumption of this unit from the +65 V dc bus is approximately 60 W and is a 1075-line raster display which produces a visible 1368 by 1024 pel display.

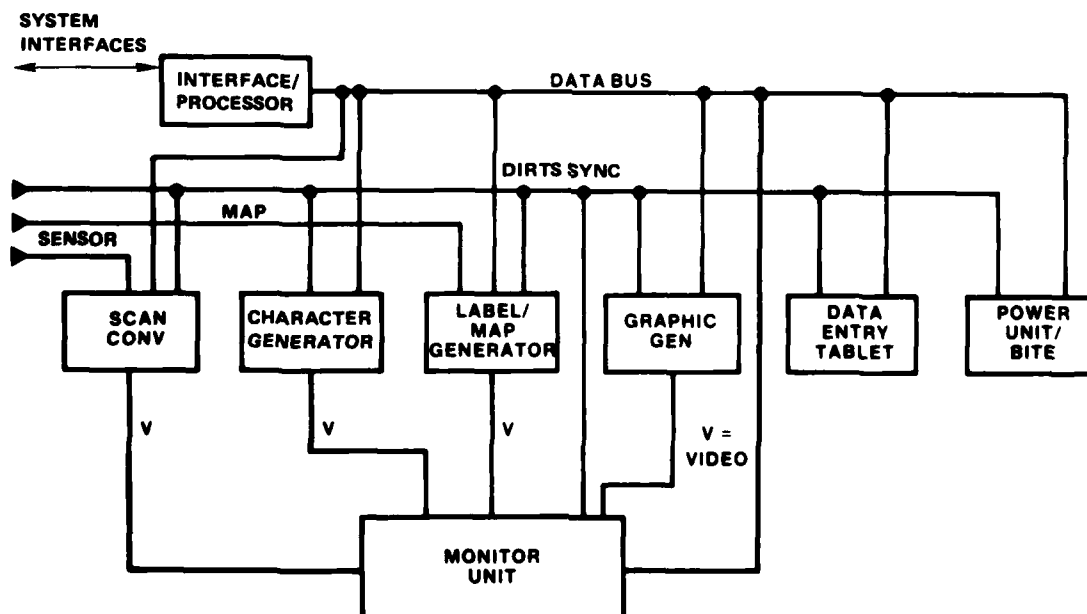


Figure 3-1. LMDS console module configuration.

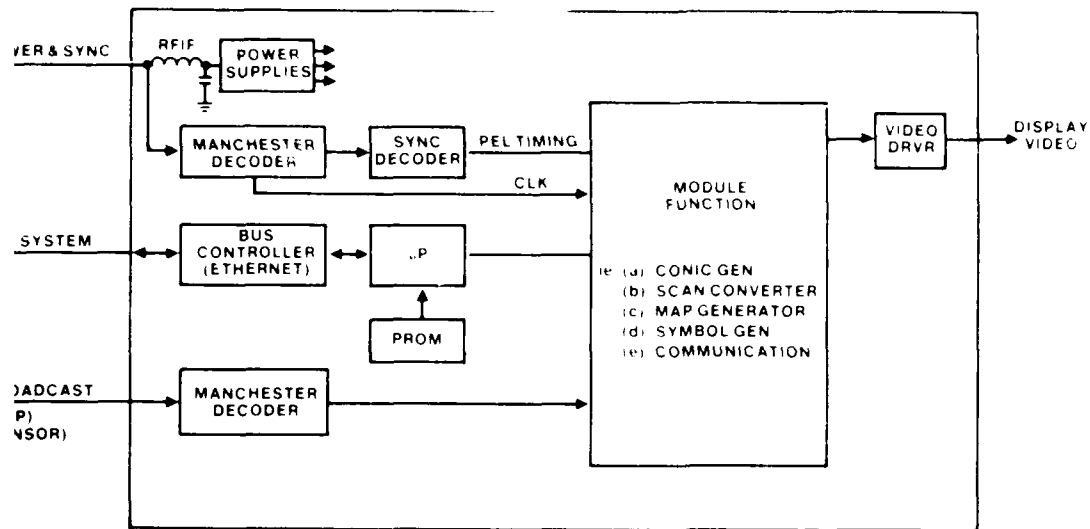


Figure 3-2. LMDS functional module block diagram.

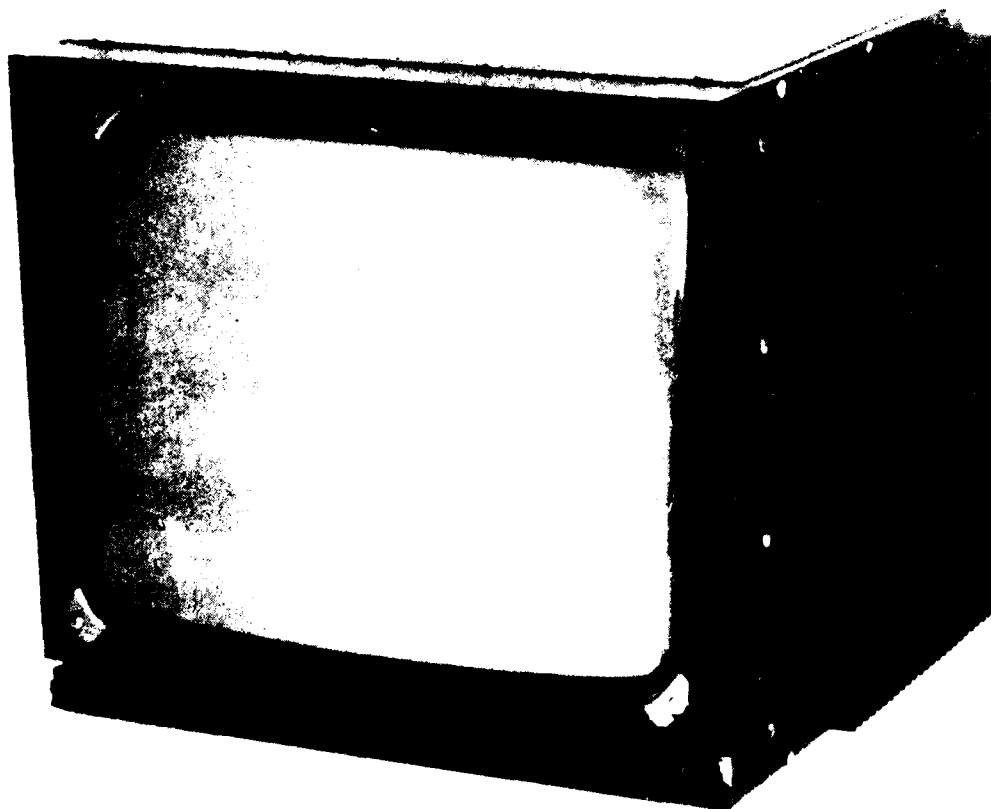


Figure 3-3. LMDS display module.

The architecture of the unit's (fig 3-4) input circuitry is based on a video table look-up ROM. The function of this ROM is to handle the brightness at the intersections of data coming from different sources. In this way, the combined brightness of a specific point does not increase with the number of coincidences of various video inputs. This technique also allows expansion to a color look-up table for use with color displays in the future.

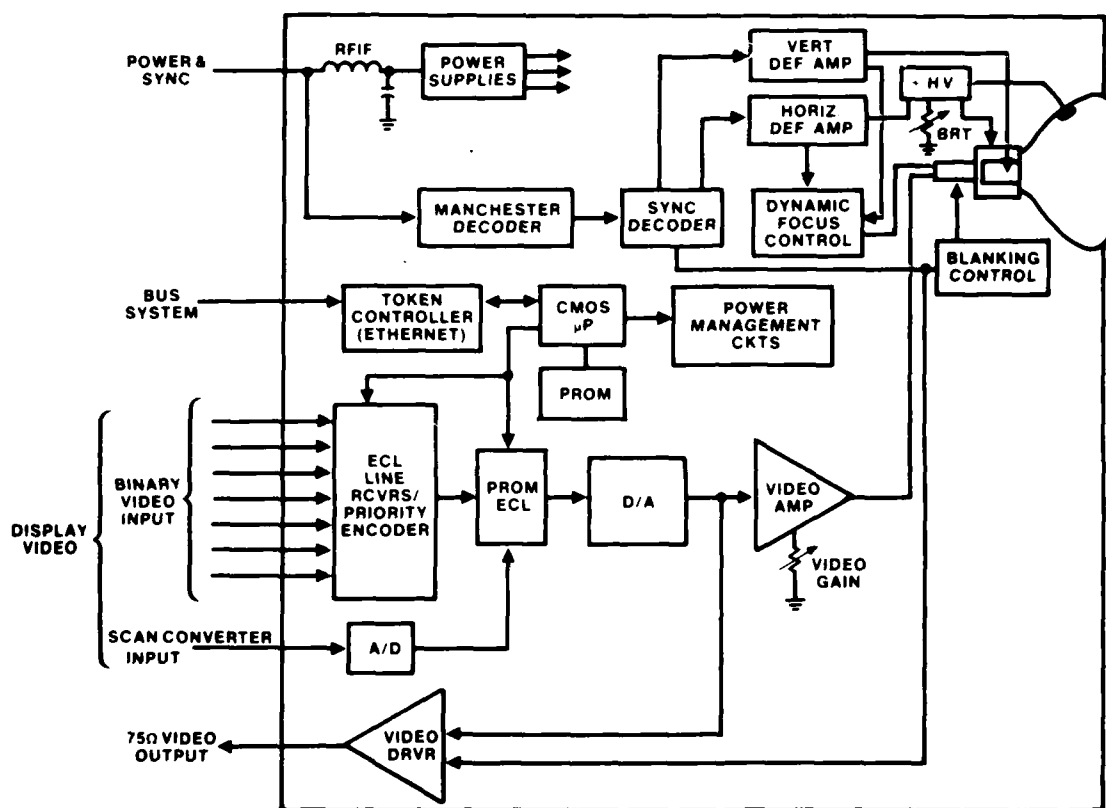


Figure 3-4. LMDS display functional block diagram.

The purpose of having the display module inputs under ETHERNET bus control is to allow operation of multiple displays on a single set of module resources, since a display operator can select any images available for construction of his display. This technique allows a number of operators to make use of the same scan converter, alphanumeric generator etc., if the range scales and offset for the system are all identical.

To minimize the number of cables between the display unit and the scan converter output, an analog input followed by an A-to-D converter is used. This keeps the scan converter interface down to a single coaxial cable between the two modules, as opposed to sending three bits of information on three independent cables.

The mechanical structure of the display unit is intended to provide support for the circuit boards on the walls of the module. Heat is then conducted to the outside air through the finned metal walls. The module's weight is expected to be 40 pounds.

#### Tablet Module

Electrically, the tablet module is divided into the digitizer tablet, a processor, a cursor generator, the input bus interface for ETHERNET, and a DIRTS decode input (fig 3-5).

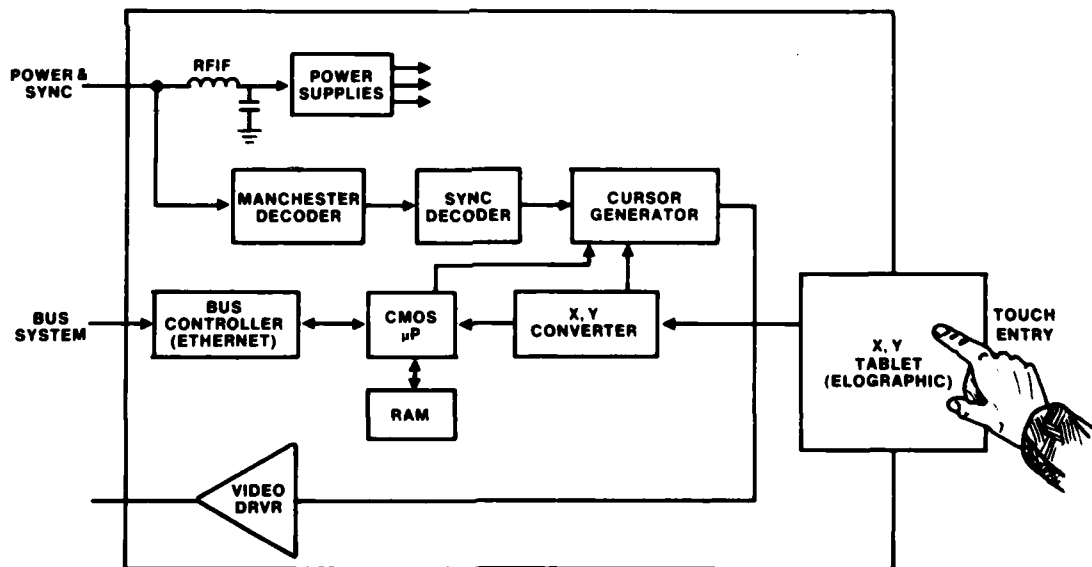


Figure 3-5. Functional block diagram of LMDS entry tablet.

The tablet module is based on a design of resistance bridging to obtain first an "X" and then a "Y" coordinate by placement of a finger or stylus on

the surface. This technique provides conversions into coordinates with a precision of about 0.004 inch. These coordinates are then sent to the processor. This processor, internal to the tablet module, interprets these coordinates in terms of instructions, commands, or mode changes depending upon the history sequence of operations on the tablet. The cursor generator unit contained within the tablet provides a convenient marker for the display's four modes: (1) a cursor would be defined for menu select or tablet label control; (2) another symbol would be used for hook function; (3) two symbols would be provided for pointers to be used from REMOTE onto DISPLAY; or (4) from REMOTE to some other DISPLAY. The cursor generator is contained within this unit to allow for rapid cursor position update. With the cursor coordinate in the unit presently being used in the image prototype version, information is sent over an RS-232 line at 9600 b/s. The resulting slow update permits a jumping effect to occur with the cursor. This type of indication in the display can be avoided by use of direct cursor control.

The tablet size in ruggedized configuration will be smaller than the unit under test. It will probably be 8.5 by 11 inches as opposed to the current size 12 inches by 16 inches pictured in figure 3-6. The power consumption for this unit is expected to be 20 W. The major reason for favoring the digitizer tablet module over the conventional trackball and switches is that there is a minimal amount of electronics and consequently less electrical power consumption necessary to satisfy the control function typically performed by switches, trackballs, and other kinds of input elements. A second reason is the splash proof surface of the tablet module, reducing the failures due to liquid spillage.

#### Intercom Unit

A standard intercom unit requires the operator to have a phone directory. What is desired in this intercom design is a unit that permits either a tree diagram or pictorial representation showing the location of phones aboard ship. This image is presented on the display, and then hooked by the operator, through the use of the tablet, so that the phone connection becomes automatic as opposed to the present digit-dialing schemes which are used to allocate the phone resources. This system also eliminates the need for

putting out phone directories since they can be entered into a central processor once, as needed, then downloaded to the various users. The intercom unit was placed on the top of the console to provide the necessary manual switching for the conventional sound-powered phone systems.



Figure 3-6. Operator using LMDS digitizer tablet.

#### Scan Converter

The scan converter module, located within the console, is the receiving element of a distributed scan converter which provides for multiuser capability. The concept behind this scan converter is the one-time digitization of the sensor for all users; this information is distributed over a single coaxial or fiberoptic cable. For small systems this would eliminate the radar switchboard unit that is required. The broadcaster portion of the multiuser scan converter contains the A-to-D and synchro-to-digital converters necessary



to digitize the sensor data and place this in a local memory. The local memory allows for scan-to-scan memory and for very rapid operator display updates for range/offset changes occurring for slowly rotating air-search radar sensors.

Rapid updating is accomplished by utilizing the local memory and by allowing the entire contents of the memory to be read out to all users in approximately 0.5 second. A typical antenna spin for an air-search radar can take 10 seconds under conditions requiring quick response to threats. This adds a burden of overhead to the processing normally done many seconds before operator reaction and decision processes can be performed. By allowing the operator to see the necessary range and offset changes that he has made within the 0.5-second interval, he will be able to make more rapid use of the system and, therefore, be able to reach his decision as to the action required much faster.

Serial broadcast of digital data also permits multisensor integration in the same cable. This is accomplished by inserting new updates from other sensors into the serial broadcast, on a noninterfere basis, with the updates from the air-search picture. The structure, therefore, by its inherent characteristics, allows the ability to overlay sensor data or do inset of sensor data. Because the information from the broadcaster has been made compact, in the sense that it is now compressed into 0.7 degree intervals and sampled in range by 4096 intervals, the conventional scan converting process at the console cannot be performed without the creation of display spoking. In some cases, the spoking and moray patterns would be so great as to preclude use of this technique. However, by using a reverse scan converting scheme which converts by selecting an X and Y coordinate on the display and asking for the appropriate "rho" and "theta" coordinate, it is possible to produce a display which is free of moray patterns.

From this brief description of the scan converter system, it can be seen that it is a versatile technique which solves a number of current system problems, reduces the amount of hardware that is required, reduces the weight and cost of cabling, and reduces the system complexity in that it eliminates a radar central switchboard for small ship applications. It also reduces the module cost by decreasing numbers of interfaces and connectors and produces a

scan converter which costs much less per console than would be required using complete conventional scan converters. This broadcaster technique also produces additional benefits by being able to create a variable persistence display and by being able to eliminate the need for long-persistence phosphors on the display. These conditions reduce the time to see an update on the display, add the capability of multisensor integration, and eliminate adjustments and control that are normally needed at the console. The unit is expected to consume 25 W and weigh less than 25 pounds at the console unit.

#### Interface/Processor Module

It is the function of the interface/processor module to perform the necessary word reformatting between the system (ie, NTDS) and the ETHERNET interbus system for the console (fig 3-7). In performing this function, the interface unit must translate word formats from the host system to the required bus word formats. The nature of the ETHERNET bus system requires that many of the word formats be rearranged and that new addressing be placed in the word formats to permit this translation to occur. The intelligence to supply these translations and manipulations of word formats is provided by a microprocessor. This microprocessor is under EEPROM control which allows downloading of test routines from bubble-memory cartridges or host processor as required. The important features of this interface unit are the ability to provide a compatible interface to the host system, the ability to provide intelligence for stand-alone capability, and the ability to provide for off-line testing. These three functions can be satisfied with minimum hardware by using the memory module with bubble-memory for reprogramming. For training purposes, the bubble-memory cartridge permits the console to be reconfigured to perform and exercise functions at simple or complex levels based on gaming techniques. The processing power needed to perform manipulations within the time constraints for the system requires a powerful microprocessing capability which may be satisfied by the imbedded AN/UYK-44 chip set.

#### Vector Generator Module

The vector generator is intended to provide all of the circles, lines, and ellipses required on the tactical display. To produce a 25 W vector

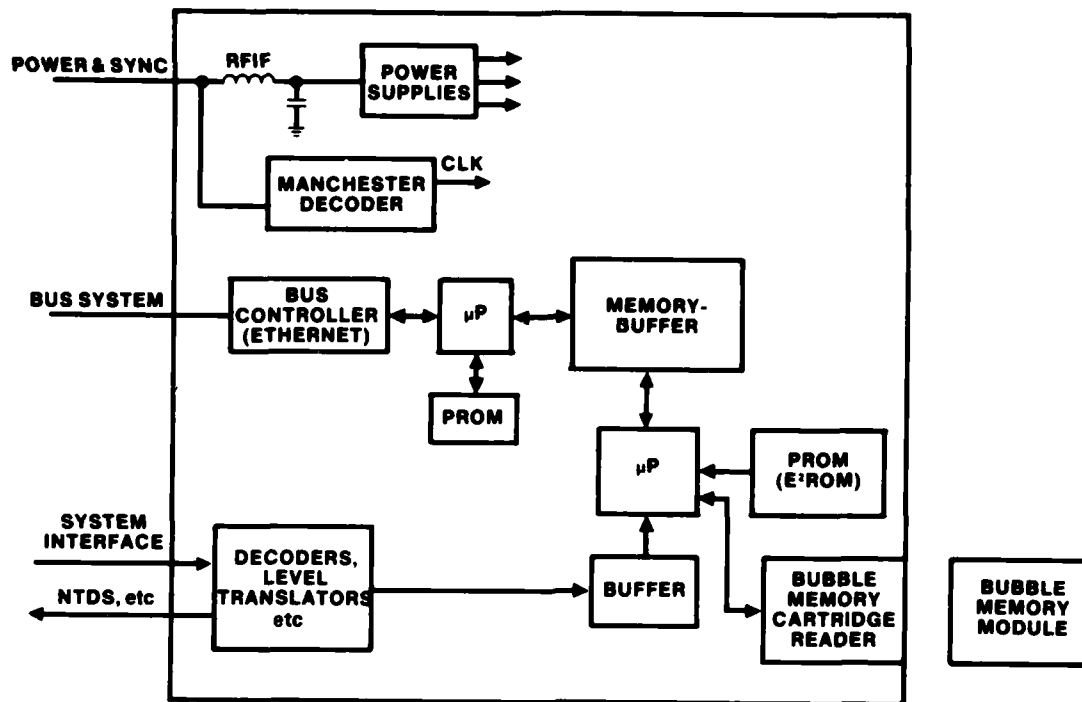


Figure 3-7. LMDS interface unit functional block diagram.

generator requires architectures and techniques considerably different from that which has been used in the past.

The vector generator architecture is based upon a microprocessor design which works in conjunction with vector generator hardware that writes into a bit-map memory. Whenever bit-map memories are used, it is difficult to move the vectors on the display without creating holidays in other vectors present. In this particular design, the problem is solved by using a background fill technique which rewrites all vectors as a background activity. Since the vector load alone is generally not very large, this technique satisfies the requirements of LMDS. A contractor has constructed and demonstrated a test unit.

#### Character Generator Module

Standard character generators make use of bit-map memories and are therefore limited in resolution to the capacity of this memory. However, the bit-

map memory technique has undesirable performance when target information from several targets occupies the same relative position on the display. The resulting alphanumeric information is not readable due to these overlaps. The best approach for a character generator design is based on an "on the fly" concept with the ability to detect collisions between information on the display and decide which symbol group should be displayed, for how long, and in what pattern. This would provide for a rotation of character groups through the conflicting area by time sequencing. The result of this process is that target information which begins to interfere would be faded into background to allow the target information to be read. A suitable time later the situation would be reversed.

Another desirable feature of this character generator approach is the method used for creation of tactical symbology. The NTDS symbol-set, when modifiers are placed on the symbols, requires a very high resolution area for symbol generation. The present concept calls for a 25 by 15 cell allocation to provide sufficient resolution to interpret these symbols with high stroke readability. To further improve the readability of this display, a technique of positioning pels on a horizontal grid of 4096 has been conceived. A simple circuit based on delay lines will allow the placement of character pels on a very precise grid to enhance readability of these symbols by removal of the "blocky" appearance of edges.

The character generator module will be capable of creating alphanumerics, upper and lower case characters with descenders and label-box definers. The alphanumeric character set which appears in the labels will be based on a 7 by 9 pel font with 3 lines of descenders. This information will be made double size or repeat field to eliminate flicker. The alphanumeric information that appears in the tactical area, for example, as tag information on a tactical symbol, will be generated in a 9 by 11 pel font. The reason for selecting this 9 by 11 pel font is to create a character that is small but highly readable to match the tactical symbol quality.

This module must also perform functions which are not normally required in a bit-map memory technique. For a raster display the character display refresh list must be ordered. Therefore, the LMDS character generator will

contain circuitry for ordering in both X and Y placement of characters. The character generator is expected to consume 25 W.

#### Map Generator Module

The map generator module is actually a component of a broadcast map system. The operation of this system is based on coding map information into Modified Fixed Word Length Run-Length Code (MFWL-RLC). Since most map applications are based on navigation requirements, a Mercator Moving Map display was considered to be the appropriate map coordinate system. This concept requires the earth to be subdivided  $2^{15}$  (32,768) on a longitude line and  $2^{16}$  (65,536) on a latitude line. By selecting a starting point on one of the longitude lines, it is possible to code the latitude lines into runs or numbers representing the distance to the next change of information. Since the principal changes occurring in this map generator involve water and land, this technique inherently provides information to define the land. The conventional techniques of writing maps are unable due to a lack of hardware fill algorithms to identify the land mass. In a complex presentation, under gain and offset modes, the operator may be completely confused by the line stroke-written map and be unable to decide which side of the lines drawn are sea and which are land. The technique used in the LMDS map generator eliminates this problem and provides a convenient method of incorporating color into the map display.

The run-length coding technique also permits high definition of land edges by changing from a truly RLC coded form to an elemental run. This technique avoids expansion of the compressed RLC data for very complex image areas. For the resolution selected, a square at the equator would define a 0.38 nautical-mile square. For most tactical operations, this resolution would be sufficient. If a very precise rendering of a specific area is required, the map generator scaling could be changed to contain only a 1024 by 1024 mile square which would result in a resolution of 94 square feet.

The final system configuration for the LMDS map generator makes use of a broadcast map generator which contains the data base for the precise mapping information in compressed form. This map generator also permits the use of

auxiliary inputs for training and accepts Global Positioning System (GPS), inputs and time log inputs so that all of the necessary navigation information needed by an operator can be nested and transmitted over the same map broadcast. Information contained within the broadcast includes: ship's latitude and longitude, time, velocity, direction, altitude, and the coded-map data as well as auxiliary information which might be based on fictitious time, velocity, direction, altitude, and map information. The map generator broadcaster transmits sufficient resolution data so that all users can select the information needed from this broadcast. Figure 3-8 shows the prototype map generator block diagram as was constructed and evaluated. Figure 3-2 shows the basic module block diagram that needs to be designed to meet this function.

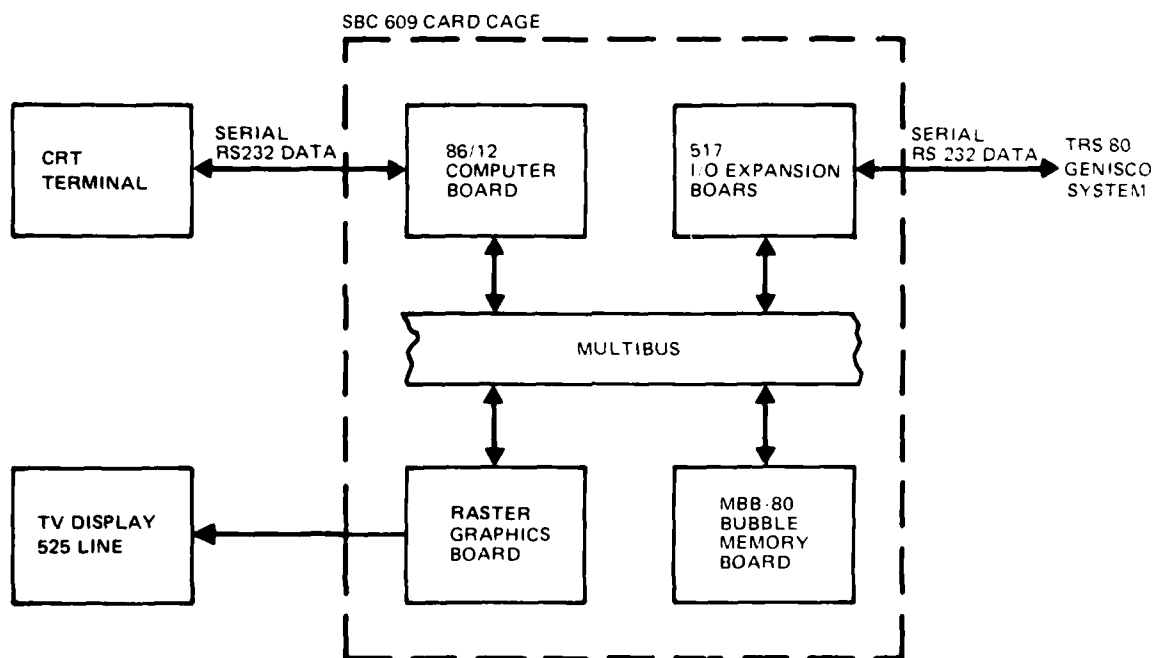


Figure 3-8. LMDS map generator block diagram.

### Power Supply Module

The function of the power supply module is to provide LMDS with power source independence. Many existing systems have distributed power supplies scattered throughout the system modules. In the event that such a system need be introduced to a new power source, all the supplies distributed throughout

the system must be changed. To avoid this, LMDS has gone to a centralized power conditioning module which filters the line power and performs line voltage regulation. This concept is depicted in figure 3-9. After line regulation, +65 V dc will be distributed to the individual modules.

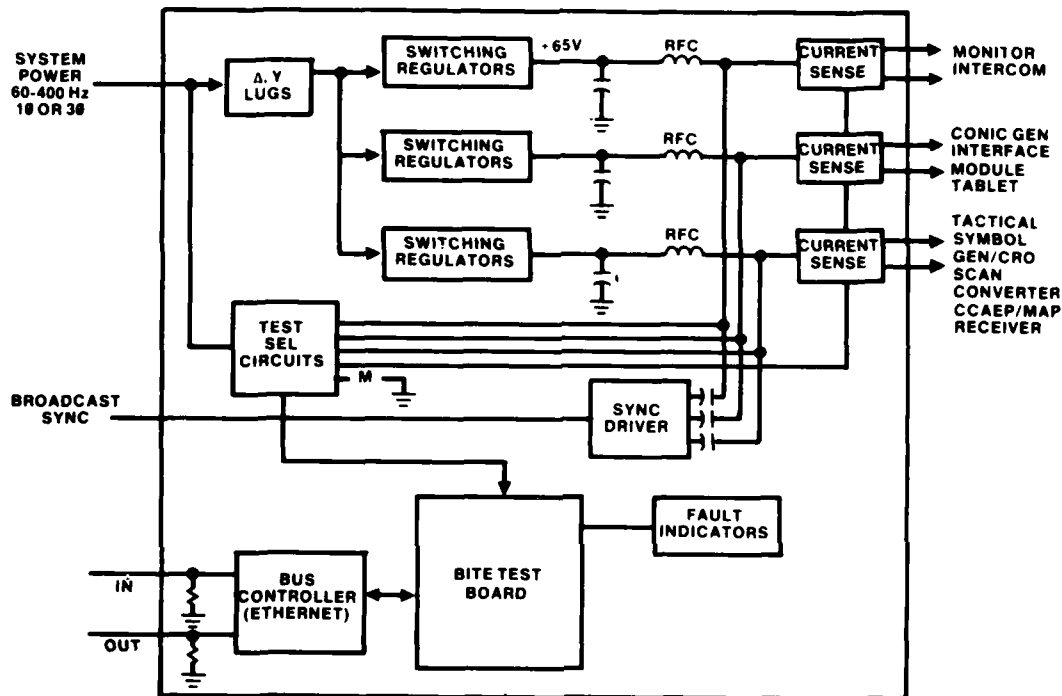


Figure 3-9. LMDS power supply functional block diagram.

The power supply is configured to handle either single or three-phase power. The use of switching regulators improves the efficiency of the power system. The individual modules that use the +65 V have switching converters which permit each of the modules to use any voltage required to suit the technologies incorporated into that module. Since all modules require power and DIRTS codes the cable which is used to conduct power to the module is also used to broadcast the DIRTS sync code. This is accomplished by suitable filter techniques which produce an equivalent 50-ohm coaxial signal carried on conductors for the power supply.

In addition to power conditioning, a built-in test processor is contained within the power supply module. It has access to input line power, 65 V dc

lines, and both ends of the ETHERNET bus. It is the function of the built-in test unit to monitor power and information exchange on ETHERNET, to announce eminent failures, if possible, and to log recurrent faults in the communications path. These fault indications are transmitted to the system through the ETHERNET bus as instructions to the alphanumeric generator. In turn, the alphanumeric generator will create appropriate messages on the display which will indicate the fault.

It is not intended that this power supply unit be a universal one, but that it only needs to be changed to move equipment from one system supply to another. The power supply unit is predicted to dissipate more than 40 W when operating a TDS console. The built-in test unit will provide a power interrupt detection message to be put on ETHERNET when power is interrupted. This will provide a message which, for future units, will allow necessary book-keeping and put-away procedures so that the system can be gracefully powered down. The total predicted efficiency for the final configuration of this system will be about 58 percent.

#### Unattended Equipment Modules

Scan Converter. The scan converter broadcaster is basically divided into two modules (fig 3-10). The purpose of this split in architecture is to provide a module set capable of being used in multiple applications. In the Tactical Display System (TDS) console configuration, the scan converter broadcaster modules which buffer the sensor to digital conversion and provide the memory function, are housed in an unattended equipment rack. This equipment rack is properly located close to the sensor to which the scan converter is allied. The most desirable configuration would be for these components to be imbedded in the radar itself.

Map Generator. The second set of unattended equipment modules comprise the map generator. Current design thinking mandates that this be a single module which would contain bubble memory chips with sufficient memory capacity to store the entire earth to the low resolution. A second module set with a floppy drive may be required in the event that high resolution/small area



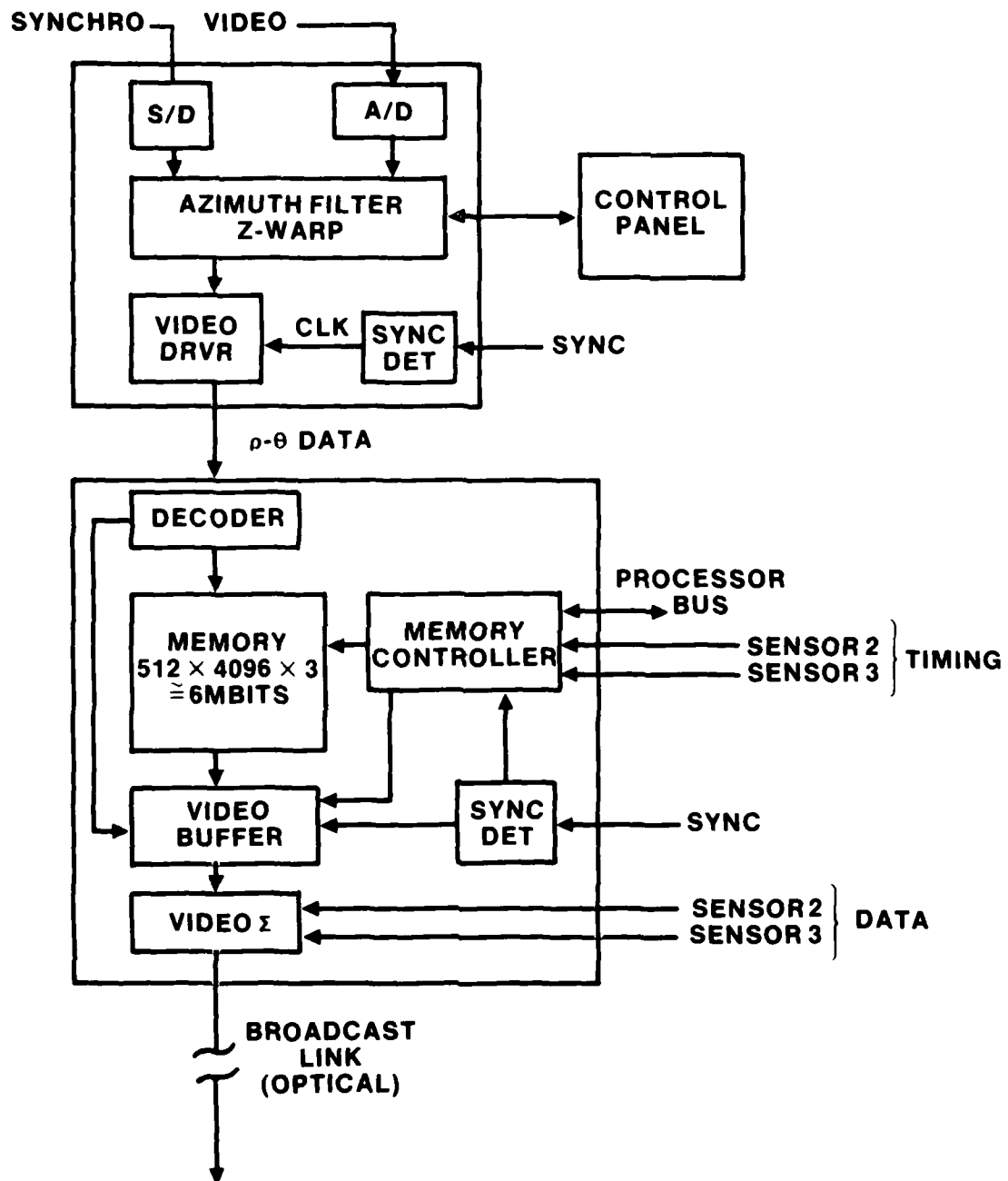


Figure 3-10. LMDS scan converter broadcaster.

s need to be downloaded to the bubble memories for a specific operation or unit could operate in conjunction with a host processor.

Digital Sync Generator DIRT Code. A special digital sync has been used MDS to avoid rise time problems inherent in standard TV sync techniques. rent in the technique for transmitting the digital composite sync information is a method of providing a 13.68 MHz system clock. From this system k circuits have been designed to derive a pel clock of 54.7 MHz.

In addition to the standard television sync characteristics features have added to the DIRT code which allow each line of the image to have its raster number, with additional fiducial points being added to the image to minimize the circuitry required in various modules. With every picture line erred, and a pel clock for each of the lines, it is possible to guarantee each of the modules within the LMDS system can create a TV image which is isely synchronized with respect to each other. Also eliminated is much uality within each of the modules that is typically dedicated to line ting and pel locations within the picture.

Junction Box/Converter. The long run serial broadcast information for scan converter and for the map generator may be transmitted on optical c. The function of the junction box/converter is to translate these cal signals into electrical signals to be distributed in local areas where e are LMDS display consoles.

#### Future Modules

Color Display. The architectural nature of LMDS accommodates a basic scheme using color for topic. This application of color to the LMDS am would display the map in one color, the tactical symbols in another, the sensor in yet another color, etc, where each module could be a ate color. In a typical system installation, it is believed that there be a large number of monochrome displays identified and only a few color lays. For this reason, if more complex arrangements of colors are needed instance colors for different types of symbology - the approach taken

would be to increase the modules of a type to satisfy that particular function until the degree of color required is met.

For the simplest color application by topic, there would be no LMDS system impact. The color monitor would replace the monochrome module. The entire change from one to the other is handled within the monitor unit by using the architecture shown for the monochrome display. The key feature is the use of the ROM video look-up table to determine intersection intensities for the various overlapping image components. When a color monitor is substituted, the color look-up table becomes the equivalent function of the ROM video table in the monochrome display.

A major problem surrounds the use of color in the tactical display within the context of available technology. The principal problem is the inability of color displays to meet either the resolution or the number of colors required. Penetration displays can provide three to four colors and maintain the required resolution in the display. Mask displays can create a greater variety of colors but are unable, at this time, to create sufficient resolution to display tactical symbols without making these symbols considerably larger than is desired to maintain display information density.

Keyboards. In applications where the LMDS system is to be used as a message terminal, a future module would be a keyboard. The digitizer tablet module is very efficient as an entry device, but is not suitable for high-speed tactile message typing. Intermediate or infrequent use of alphanumerics can be performed by use of a menu select scheme.

Slow Scan Display Transmitter. To allow display images to be transmitted to a remote location, it may be desirable to have within the unit a module capable of dissecting the summed video output of the monitor. Store this image in a bit-map memory in compressed form suitable for relatively rapid transmission over narrowband communication systems. If this unit were capable of bilateral transmitting and receiving, an LMDS console could be used to transmit over standard communication systems an image which could be received and redisplayed on another LMDS console.

### Unattended Equipment

Radar Recorder. The ability to record images collected by radar on video magnetic tape permits playback of entire Fleet operations at a later date. This could be a valuable tool for Fleet operations, analysis and debriefing from exercises.

Digital Bus Recorder. To provide the equivalent capability, a bus recorder for ETHERNET would permit regeneration of the entire scenario. This is a capability that may be added at a later date.

Video Sensor Simulation. The ability to place equivalent video into the system for operations and training performed within a harbor region, without emitting from the radars or sonar, might make use of the video sensor simulator.

Sensor Switchboard. Even though the LMDS provides a method by which sensors can be summed onto a single sensor distribution cable, large numbers of sensors (<5) (five) require more than one cable. In such a case, to direct the appropriate information to the correct user based on his request, a digital sensor switchboard must perform the necessary connections. Because of the serial nature of the broadcasts, this module can be a single LMDS module in size and power.

## SYSTEM CONFIGURATION AND SPECIFICATIONS

### SPECIFICATIONS

<u>FEATURE</u>	<u>CHARACTERISTICS</u>
RELIABILITY:	
Shipboard-installed at 50°C	MTBF of 2000 hr
MAINTAINABILITY:	
Cable accessibility	Front access
Module accessibility	Front access

## SPECIFICATIONS (Continued)

<u>FEATURE</u>	<u>CHARACTERISTICS</u>
Built-in test	System level and modular level for monitoring out-of-tolerance voltages, over-temperature, and test patterns
Troubleshooting	Unit can be dismantled by one person for installation. Standard test equipment.
<b>ELECTRICAL CONSTRUCTION:</b>	
Power module	Conducted power line control Operating parameters: 40-400 Hz 95-125 Vac (single or 3-phase y or $\Delta$ ) 250 W total power delivered
<b>MECHANICAL CONSTRUCTION:</b>	
Resistance to environment	Splash-proof, modules RFI sealed
Installation	Rigid-mounted to deck with 4 bolts
Shock and vibration	Meets MIL-STD-167-1 for resonances greater than 50 Hz and MIL-S-901C for high impact shock
Control surface layout	Per MIL-S-1472
Operational light ambience	To 1000 fc with matched filter display and P-43 phosphor
<b>HIGH RESOLUTION MONITOR:</b>	
Screen	15-inch diagonal screen
Resolution	1024 x 1368 pels
Type	1075-line TV standard 2:1 interlace
<b>HIGH RESOLUTION GRAPHICS:</b>	
Graphics module	Microprocessor bit-map organization 1024 by 1024 pel
Created display list	Vectors and vector renderings of hyperbolas, circles, parabolas, and ellipses

# SPECIFICATIONS (Continued)

<u>FEATURE</u>	<u>CHARACTERISTICS</u>
Line format	Solid, dashed, dotted, with scaling, offset, and scissoring
HIGH RESOLUTION SYMBOL GENERATOR:	
Symbol fonts	7 x 9; 7 x 9 double size; 9 x 11; 9 x 11 double size; NTDS symbology in 15 x 25 and 30 x 50
Blink	At 2 Hz
Display dimensions	80 character/line; 32 lines
Label symbols	Alphanumerics 7 x 9 double size with descenders 7 x 12 double size
SCAN CONVERTER, DISTRIBUTED:	
Broadcast converter processing	8 bits; 512 fixed-azimuth (0.7°) increments; 4096 range increments
Serialization	Multiple sensor. Manchester encoded
Broadcast update time	0.5 second without other sensors
Console scan converter	Process range scale offset
Operator selectable video	Uses reverse scan conversion technique
INTENSITY, MONITOR AND CONTROL:	
High resolution monitor	Video look-up table 15kV, 10 mil spotsize 20 ft-L screen brightness P-39 phosphor
System organization	Color separate video from each module
DISPLAY PROCESSOR:	
Processor compatibility	AN/UYK-20; AN/UYK-14; AN/UYK-44; AN/UYK-7
I/O options	Per MIL-STD-1397A; NATO STANAG 4153; ETHERNET; RS-232; specials

SPECIFICATIONS (Continued)

<u>FEATURE</u>	<u>CHARACTERISTICS</u>
PHYSICAL CHARACTERISTICS:	
Weight	250 lb (predicted)
Dimensions	48 inches high, 26-3/4 inches wide, 34 inches deep
Framework	Easily customized
HIGH RESOLUTION MAP GENERATOR:	Reproduces world maps to .38 nautical mile square Requires external map source Interfaces to 13.68 MHz Manchester encoded serial bus.
TABLET ENTRY MODULE:	
Entry	Finger or stylus for control and menu selection positional accuracy to .004 inch size 11.5 inches x 15 inches active area.
CURSORS:	
Quantity	4 different cursors in display
Type	Local operator, hook, remotely pointing, remote pointing.
SERVICE CONDITIONS:	
Operating temperature range	0° to 50°C Ambient Air
Operating relative humidity range	0 to 90 percent
Vibration	Per MIL-STD-810
Shock	Per MIL-STD-901
Transportability	Sea level to 40000 ft
Operating altitude range	Sea level to 10000 ft

## SYSTEM OPERATION

With the capabilities outlined in the previous module descriptions, some new and important improvements in system operation can obviously be achieved. For the first time, the operator is not required to remove his attention from the display. This display now looks much like a window into an information space which contains control information, sensor information, status information, and tabular data. With the limited amount of display space available for labels, an advantage is created by not having controls on the display which can permit illegal operations. This will reduce the likelihood of operator error, reduce training time, and reduce life-cycle cost. For the first time, with an LMDS system, it will be possible to create multiple sensor overlays including EW and ASW information overlaying detailed map information. This creates a variety of exciting possibilities for maximizing detection and minimizing intercept.



SECTION 4  
APPENDICES

## APPENDIX A

### TABLET VS TRACKBALL COMPARATIVE TEST DATA

#### INTRODUCTION

This report discusses an experiment which was conducted to investigate the comparative performance of two tracking control devices. The devices are under consideration for application in Navy command and control consoles. One device, a trackball, has been widely used in previously developed command and control consoles; whereas the other device, a pressure-sensitive digitizer tablet and a more recent invention, has seen limited prior use, principally as an input device to graphic displays. The experiment discussed here compares operator performance in terms of response time and error rate for each of the devices.

Command and control consoles generally include a display upon which a movable cursor is superimposed. The cursor is used to designate a point or symbol on the display for a wide variety of purposes, such as track position or classification updating. Many different devices have been used for positioning the cursor, including light pens, movable joysticks, isometric joysticks, and trackballs. Of these, the trackball has generally shown good comparative results when tested. Comparable performance tests between the digitizer tablet and other tracking control devices is not available in the literature. Therefore, this test was performed to determine the relative performance of the digitizer tablet.

#### METHOD

#### EQUIPMENT

The display equipment was a 17-inch CONRAC TV monitor of high resolution (1024 x 1024). Symbology was generated by a Genisco display unit programmed as a signal generator. The two tracking devices used were: (1) a pressure-sensitive digitizer tablet, having a sensitized area of 11.5 inches by 15

inches, manufactured by Elographics, Inc; and (2) a 4-inch diameter trackball, manufactured by Orbit Industries Corp. Both tracking devices were capable of high resolution control. The experimental program was controlled by a Tandy Corporation TRS-80 microcomputer with five 5-1/2-inch drives used for program loading. A printer was connected to the microcomputer and used to record the results of each completed trial of 48 events. An equipment block diagram is shown in figure A-1.

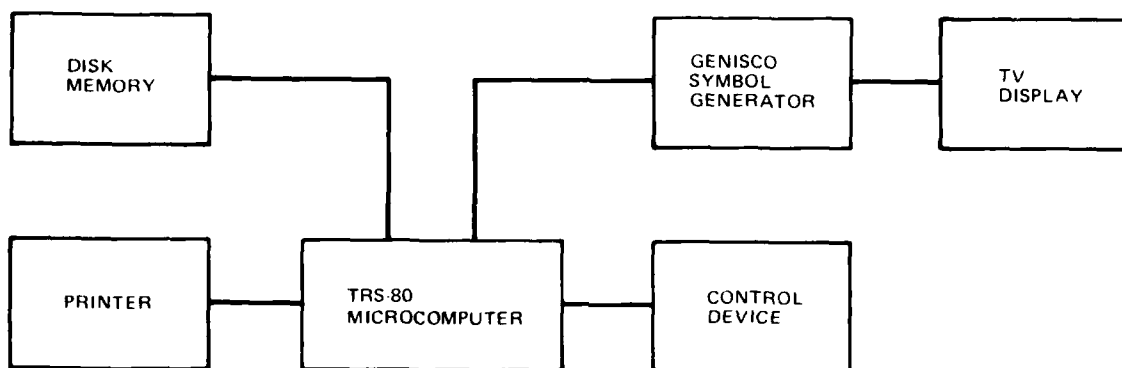


Figure A-1. Equipment block diagram.

The following discussion details the approach and results of a comparability test between an NTDS-TDS trackball and a pressure-sensitive digitizer tablet.

#### **SUBJECTS**

A total of 16 subjects were used during the experiment. Eight of the subjects were highly trained military operators of Navy command and control (CIC) consoles, and, hence, experienced in the use of the trackball tracking device. The remaining eight subjects were civilian scientists and engineers, none of whom were experienced with the trackball. All subjects were untrained in use of the digitizer tablet. All were volunteers.

## TASK AND PROCEDURES

The subjects to be tested were scheduled to report individually since the entire procedure with each tracking device required almost 2 hours to complete. The testing with each device was scheduled separately. On reporting, the subjects were given an instruction sheet which explained the purpose of the experiment and attempted to establish a common frame of reference. Procedures were described and the subject was instructed to place equal stress on tracking, accuracy, and speed of response.

The task involved the presentation of a target symbol at a pseudorandom location of the display. The symbol was a circle, slightly less than 1/8 inch in diameter. It was presented at high contrast with the background and was immediately apparent to the subject when it appeared. Thus, search time was negligible. The appearance of the cursor, a cross, depended upon the type of tracking device used. When the digitizer tablet was used, the cursor appeared at a corresponding location on the display when pressure was applied. Subjects were instructed to use either stylus or fingertip, as preferred, and to move the cursor until it became superimposed over the target symbol. The preferred hand was used when tracking with the digitizer tablet. When the trackball was used, however, the cursor appeared in the center of the display simultaneously with the target symbol. Only the right hand was used for tracking, due to the placement of the trackball (similar to operator console). Tracking procedures were similar. After the cursor was superimposed over the target the event was entered, that is, recorded. Again, entry procedures varied slightly depending upon the tracking device. With the digitizer tablet, event entry was made by releasing pressure at the target area and reapplying it at one of two designated corners of the tablet. Normally, entry was made with the hand opposite to the tracking hand. With the trackball, however, entry was made by pressing a switch adjacent to the trackball. Following the event entry, the computer recorded the response time interval between target presentation and entry and error distance between target center and cursor center.

Each event, consisting of target presentation (at a pseudorandom location), tracking, and entry, was followed immediately with another target presentation, etc. A trial consisted of 48 such events. Figure A-2 shows the target presentation order and relative location on the display. Although the order of presentation remained fixed for all trials, each trial was commenced at a random point in the series. This gave the subjects the impression that the events and trials were indeed random presentations. Target positions were pseudorandom, tabulated and read in sequence from a random starting point. Following each trial, the subject was allowed to relax for a few minutes while data printouts were made and reviewed.

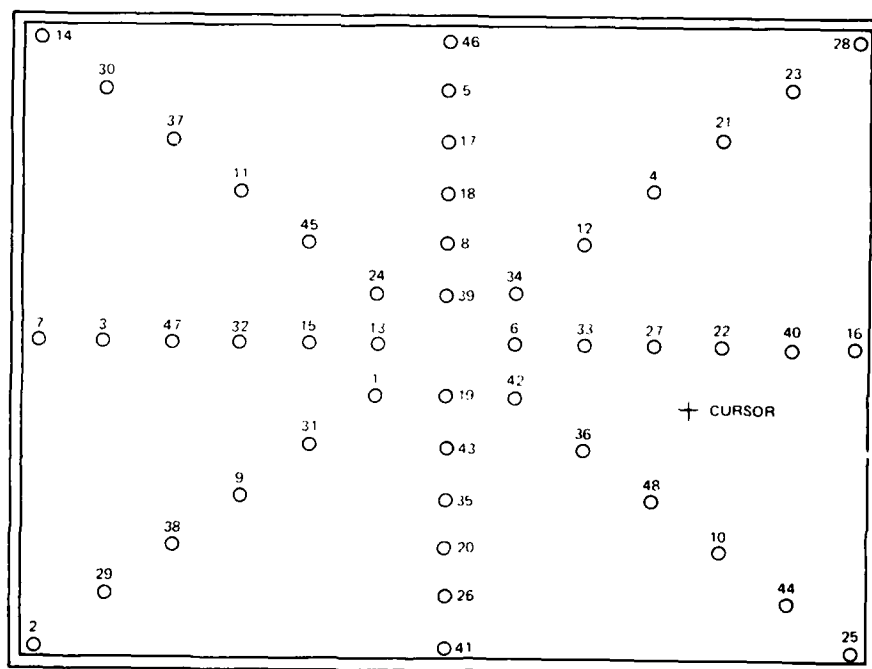


Figure A-2. Target presentation order and position.

Each subject testing session consisted of five training trials followed by 10 test trials, each consisting of 48 tracking events. The five training trials proved to be more than adequate for attaining proficiency, even for subjects untrained in either device. Performance approached an asymptote well before the fifth training trial was completed.

## EXPERIMENTAL DESIGN

The experimental design used was the repeated measures equivalent materials design. This design is illustrated in table A-1.

Table A-1. Repeated measures equivalent materials design.

Devices	PERFORMANCE MEASURES (RESPONSE TIME; ERROR)			
	Digitizer Tablet		Trackball	
	CIC-TRAINED	UNTRAINED	CIC-TRAINED	UNTRAINED
SUBJECTS	1 . . . 8	1 . . 8	1 . . . 8	1 . . 8
1	.	.	.	.
.	.	.	.	.
TRIALS .	.	.	.	.
.				
(ea 48 .				
events) 10				

The independent variables are the digitizer tablet and the trackball control devices. A classificatory variable in this experiment is prior subject training ie, CIC-trained (trackball experienced) versus untrained (no or minimal trackball experience). This variable was tested for purposes of determining the effects of long-term training and experience with the trackball. Regardless of prior training, subjects in both categories received five training trials with each device prior to testing.

The dependent variables are the performance measures: response time and error. Response time was measured from initial target presentation to entry response. Error was measured from the target center to the cursor center at the time of entry. Time measurement was made automatically by the microcomputer and was recorded in units of seconds and hundredths of a second. Error measurement was also made automatically by the computer and was recorded in units of picture elements or pixels (pixel  $\approx$  0.085 in.) The pixel was a convenient unit of measurement since the symbols and target locations were programmed in pixel units; thus, the computer was capable of precise error measurement.

## RESULTS AND DISCUSSION

### TRACKBALL VERSUS DIGITIZER TABLET

The general purpose of this investigation was to determine comparative tracking performance using the pressure-sensitive digitizer tablet and the trackball for application to LMDS. Results are shown graphically in figures A-3 and A-4, in which the data from all subjects are pooled.

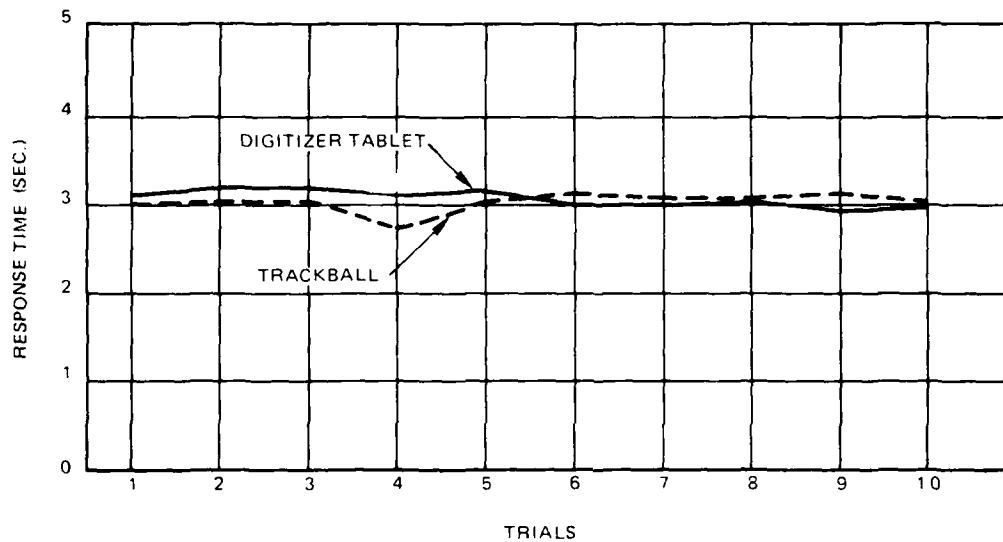


Figure A-3. Mean response times for all subjects.

The experiment was designed to compare the performance of the trackball to the digitizer in the application to LMDS. This is different from comparison of the trackball as is applied to existing TDS consoles to the digitizer tablet as applied to LMDS. The distinction places the trackball in a more favored position due to the nature of the method of range scaling in LMDS. The trackball due to the method of accumulating incremental change pulses with motion is typically very slow on longer range scales. When applied to the LMDS the speed effective for the trackball as compared to a TDS console is approximately the speed range of the 1 nautical mile scale.

Average response times for both devices were the same or approximately the same - about 3 seconds per tracking event. Statistically, there was no

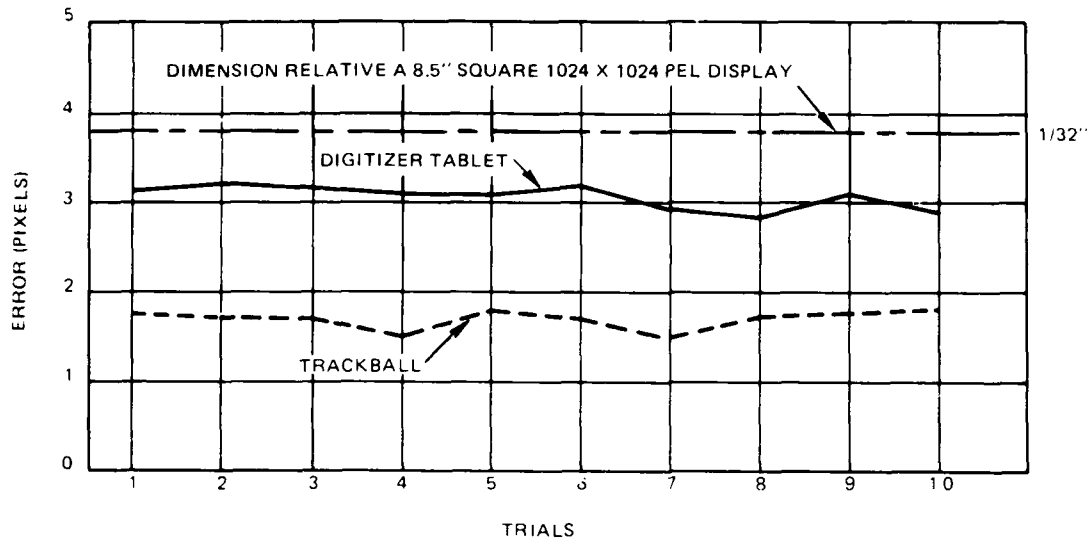


Figure A-4. Mean error of all subjects.

significant difference in response times between devices ( $p > 5\%$ ). Some subjects were faster trackers than others; the fastest tracker averaged about 2 seconds per event, whereas the slowest tracker averaged about 4 seconds per event. The fastest trackers with the digitizer tablet tended also to be the fastest trackers with the trackball.

Comparative tracking error with the two devices is shown in figure A-4. The figure shows that the average error per tracking event is consistently greater when using the digitizer tablet than when using the trackball. With the digitizer tablet, mean error was about 3 pixels; with the trackball, the mean error was about 1.7 pixels. Differences were consistent and statistically significant ( $p < 1\%$ ). Although the pixel was a very small unit (pixel  $\approx 0.085$  in) it was discernible. There is little doubt that error could have been further reduced for either control device had the subject chosen to ignore response time as a factor in performance.

An explanation for the better tracking accuracy performance of the trackball compared to the digitizer tablet can only be found through further investigation. Two factors are thought to be major contributors to the differences in performance. First, the precision control characteristics of the trackball appear better and easier than those of the digitizer tablet. At least some of



this can be attributed to how the tracking hand and arm were stabilized. When using the trackball, the tracking hand was stabilized or anchored by placing the heel of the hand at the base of the trackball and rotating the ball with the fingers. However, when tracking with the digitizer tablet, the tracking arm was usually anchored at the elbow, thus making fine control more difficult. A second factor which may have contributed to a larger digitizer tablet error was a slight shift in the pressure centroid as finger pressure was removed. A slight shift in the pressure centroid caused the cursor to move off the target and only when pressure was released vertically did the cursor remain fixed until its position was entered. This shift may be reduced by software filtering of the last data point announced to the microcomputer, or by programming the microcomputer to discard the changing data points just preceding the removal of pressure from the tablet.

#### SUBJECTS: CIC-TRAINED VERSUS UNTRAINED

Performance of the two different groups is shown in figures A-5 and A-6. It is apparent that some differences occur due to training and/or selection.

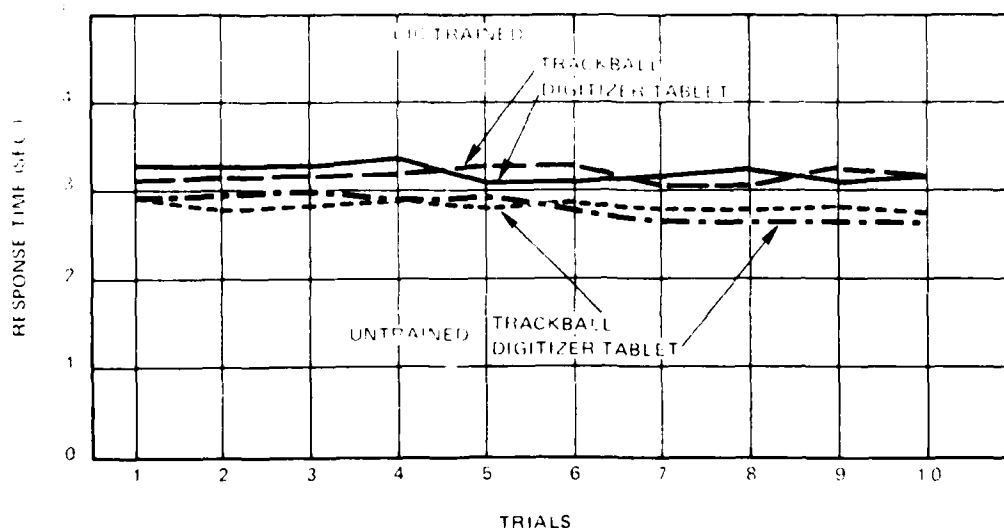


Figure A-5. Mean response times for CIC-trained and untrained subjects.

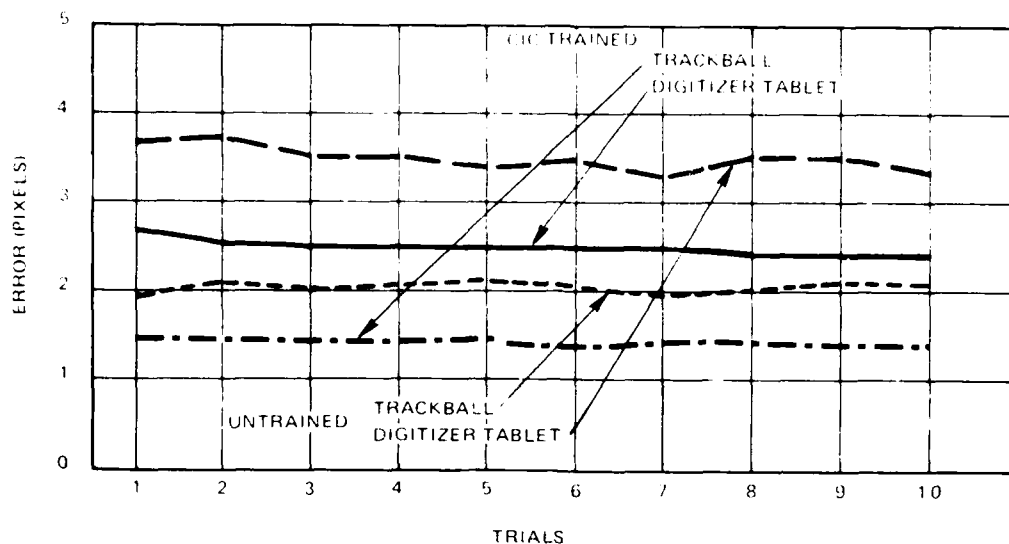


Figure A-6. Mean errors for CIC-trained and untrained subjects.

The mean response times for the two groups were near the same value, about 3 s per event, although the mean response times for CIC-trained subjects were consistently longer than for untrained subjects. However, the differences were not statistically significant ( $p > 5\%$ ) due to high intragroup variability.

The tracking error performance of the two groups was highly different - the lowest mean error being made, with both devices, by the CIC-trained group. Differences were statistically significant ( $p < 5\%$ ) although some performance between groups overlapped.

It seems reasonable to assume that the CIC-trained group approached the tracking task with a somewhat different viewpoint than the untrained group, regardless of the fact that both groups were instructed to consider speed and accuracy as equally valued aspects of performance. The CIC-trained group was consistently more accurate not only with the trackball with which they were familiar but also with the digitizer tablet. Their mean response time was also slightly slower with both devices, thus indicating a greater emphasis on accuracy than on speed. An increased bias toward accuracy may readily have stemmed from CIC training, where accuracy in track position updating is an important aspect of the CIC task.

## ANALYSIS OF VARIANCE

An analysis of variance was made for each of the dependent variables: response time (speed) and error (accuracy). The results are shown in tables A-2 and A-3.

Table A-2 shows the analysis of the response time variable. None of the tests showed a level of significance equal to 5 percent or better. The largest variability occurred between the two subject groups, thus supporting what is apparent in figure A-5.

Table A-2. Analysis of variance: response time.

Source of Variation	Degrees of Freedom DF	Sum of Squares SS	Mean Square MS	F	Proba- bility P
Between subject groups	15	5.88			
CIC-trained vs untrained	1	0.8	0.8	2.22	NS
Total between groups error	14	5.08	0.86		
Within subjects	16	2.76	0.17		
Trackball vs digitizer tablet	1	0.0	0.0	0.0	NS
Interaction: devices vs training	1	0.01	0.01	0.05	NS
Total within subjects error	<u>14</u>	<u>2.75</u>	0.2		
TOTAL:	31	8.64			

Table A-3 shows the analysis of the performance error variable. Two tests pass the accepted measure of significance. The difference between CIC-trained versus untrained subjects was significant at the 5 percent level of confidence. However, the difference between trackball and digitizer tablet was significant at the 1 percent level. These differences are readily supported by figure A-6.

Table A-3. Analysis of variance: error.

Source of Variation	DF	SS	MS	F	P
Between subject groups	15	13.865	-	-	-
CIC-trained vs untrained	1	5.08	5.08	8.06	<0.05
Total between groups error	14	8.785	0.63	-	-
Within subjects	16	19.175	1.2	-	-
Trackball vs digitizer tablet	1	13.585	13.585	35.75	<0.01
Interaction: Devices vs training	1	0.255	0.255	0.67	NS
Total within subjects error	<u>14</u>	<u>5.335</u>	0.38	-	
TOTAL:	31	33.04			

#### CORRELATION OF VARIABLES

One would generally expect the performance variables, response time, and error to be correlated to a negative degree. That is, we would generally expect the faster response to be related to larger error, and vice versa. A marksman firing rapid fire usually has a lower score than when firing slow fire, etc. To examine the relationship between variables, a Pearson's Product Moment correlation was computed on the performance variables for each device. The results showed that when using the digitizer tablet there was a low negative correlation between response time and error size ( $R = -0.23$ ). However, when using the trackball there was a high negative correlation between response time and error size ( $R = -0.71$ ).

Correlation coefficients were also computed for subjects versus each of the performance variables. Subjects' response time performance on the tracking devices was moderately correlated ( $R = 0.43$ ). However, subjects' error performance on the two devices was somewhat more highly correlated ( $R = 0.58$ ).

#### CONCLUSIONS AND RECOMMENDATIONS

Under the conditions established for the study herein, tracking performance with digitizer tablet and trackball was comparable for speed and

favorable to the trackball for accuracy. Accuracy differences were highly significant. There was some evidence that the two subject groups were not representative of the same subject population. The CIC-trained group appeared to emphasize tracking accuracy at some cost of reaction time as compared to the untrained group. However, group differences were not highly significant.

The ultimate objective of this study and related investigations was to determine the suitability of the digitizer tablet for possible application in Navy CIC consoles. Of course, such a determination must be based upon broader considerations than tracking performance only. Target tracking, in terms of speed and accuracy parameters only, is a relatively minor part of the application of such control devices. A more common application is to use the control device to designate a track symbol for amplifying information readout or updating, or to select an option from a display or control "menu," etc. With such applications, there is no requirement for the degree of tracking accuracy demonstrated by either of the devices under study. Target positioning and position updating are the principal functions for which tracking accuracy is a valuable attribute. However, with the advent and increased use of automatic detection and tracking capability in radar systems, manual target tracking is expected to become a seldom-used capability in future command and control centers. Thus, the changing functions of control devices require reassessment of priority of attributes. Tracking accuracy is likely to become less important. The accuracy demonstrated with the digitizer tablet appears to be adequate to meet the operational requirements of Navy CIC consoles and specifically the design goals of LMDS.

The pressure-sensitive digitizer tablet is recommended for further investigation as a candidate control device for CIC consoles. In addition to the comparisons already made, the digitizer tablet appears to offer advantages over the trackball in the following areas:

- A. When integrated with computer technology, the digitizer tablet can be used flexibly to control a variety of control functions, such as multiple fixed-function actions in addition to cursor tracking, whereas a trackball or joystick would require the addition of other control devices to achieve a comparable capability.

- B. It contains minimal moving parts and, therefore, appears to be less susceptible to wearout and failure.
- C. It can be sealed and made impervious to dirt or spilled liquids.
- D. It is likely to be more economical to procure and maintain.

## APPENDIX B

### LMDS MODULE ASSEMBLY THERMAL DESIGN SUMMARY

#### INTRODUCTION

LMDS thermal design was approached in three phases. Initially, a feasibility study was conducted to evaluate the proposed module natural convection cooling system thermal design. The feasibility of various cooling system configurations was explored and preliminary thermal design goals and requirements were established.

Secondly, a more detailed computer-aided thermal analysis was performed on the preliminary design configuration of a module heat sink and circuit board assembly. The results of the analysis predicted temperatures that supported original assumptions regarding the feasibility of the design concept. The analysis also indicated potential problem areas in the natural convection cooling system that will require particular attention during the detailed design process.

Finally, thermal tests were performed on an engineering model of a module assembly using typical heat sinks and simulated printed circuit boards. The experimental data indicate reasonable correlation with the computer analysis and support the original assumptions used to construct the thermal model.

#### PRELIMINARY DESIGN STUDY

A preliminary steady-state thermal analysis was performed on the conceptual LMDS system design to determine whether the configuration would meet the thermal design requirements. The proposed design utilized natural convection and conduction as the primary cooling method for console electronics. Other cooling techniques such as forced air, liquid, or heat pipes would be considered if natural convection could not meet the system design requirements under worst case conditions. This is a departure from conventional designs that normally require more complex and less reliable fans or heat exchanger

systems to provide temperature control. Natural convection offers the simplest, most reliable, and least costly system. Other parameters considered in the selection and design of a cooling system include part temperature limits, environmental conditions, reliability, weight, space, heat concentrations, and life cycle costs.

The thermal analysis was based upon natural convection cooling and estimated heat loads. The results of this analysis indicate that a natural convection cooled design is feasible if sufficient space is available for heat dissipating surfaces and adequate heat conduction paths can be maintained.

#### COMPUTER THERMAL ANALYSIS

A detailed computer thermal analysis of an electronic module was made to evaluate whether or not the natural convection cooling could maintain electronic part temperatures within allowable design limits. Part junction temperatures were estimated by superimposing part temperature increases on average board temperatures predicted by the computer model.

The Systems Improved Differencing Analyzer (SINDA) computer program and a UNIVAC 1110 computer were used to predict thermal model temperatures. The SINDA thermal analyzer program was designed for a wide variety of steady-state heat transfer problems.

The thermal analysis was based upon the following assumptions and conditions:

- a. Steady-state heat transfer (transient conditions during warmup were not considered).
- b. Natural convection and conduction are the primary heat transfer modes.
- c. Radiation and internal natural convection were neglected.
- d. Heat dissipation was uniformly distributed across the circuit 10" x 15" board at a nominal 12.5 watts.
- e. Material thermal properties are constant with temperature and are as follows:



<u>MATERIAL</u>	<u>THERMAL CONDUCTIVITY BTU/HR-FT-°F</u>
Aluminum	100
Copper	220
Fiberglass	0.15
Air	0.016

- f. Ambient air temperature was 50°C.
- g. Circuit board nominal joint interface contact resistance was 1.25°F-hr/BTU/per No. 6-32 screws.
- h. The external natural convection heat transfer coefficient was constant over the surface of the heat sink fins and was 0.49 BTU/hr-°F-ft<sup>2</sup>.
- i. Heat sink temperature gradients are negligible.

#### DESCRIPTION OF COMPUTER MODELS

A detailed thermal model was made of a symmetrical section of a typical electronic module that included a heat sink and printed circuit board. The model node geometry is shown in figure B-1. The heat flow paths and circuit board mounting details are shown in figure B-2 and B-3. The B-3 version was modified to eliminate the milling operation shown. The tested configurations have an additional thermal interface which is shown in figure B-15.

The thermal model of the circuit board was conservatively designed to predict peak temperatures and temperature gradients. The board was divided into 150 nodes that represented small elements of the board. The temperature was assumed constant throughout each node. The nodes were interconnected by thermal resistors that represented conduction heat flow paths across the board, through the attachment points, and into the heat sink base. Each node represented an area on the board that was expected to be occupied by an electronic component. Heat was uniformly applied across the board at the center of each node.

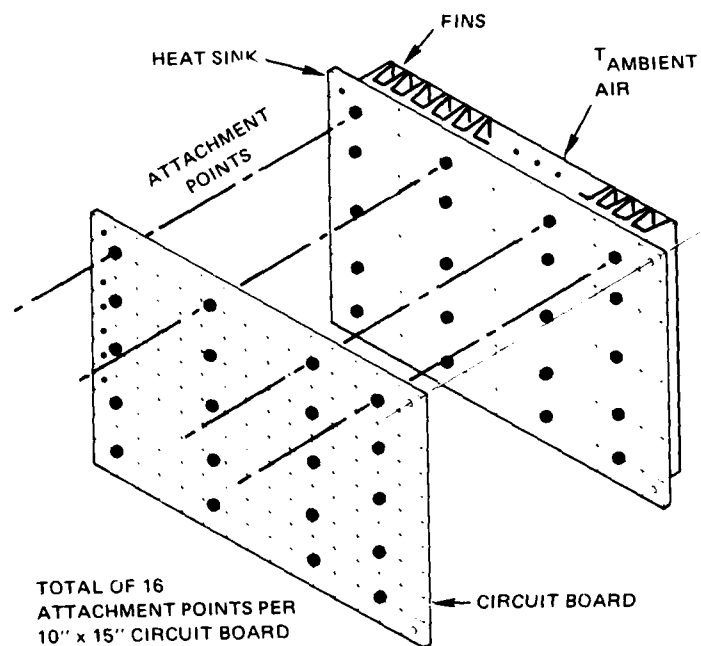


Figure B-1. LMDS module thermal model nodal arrangement.

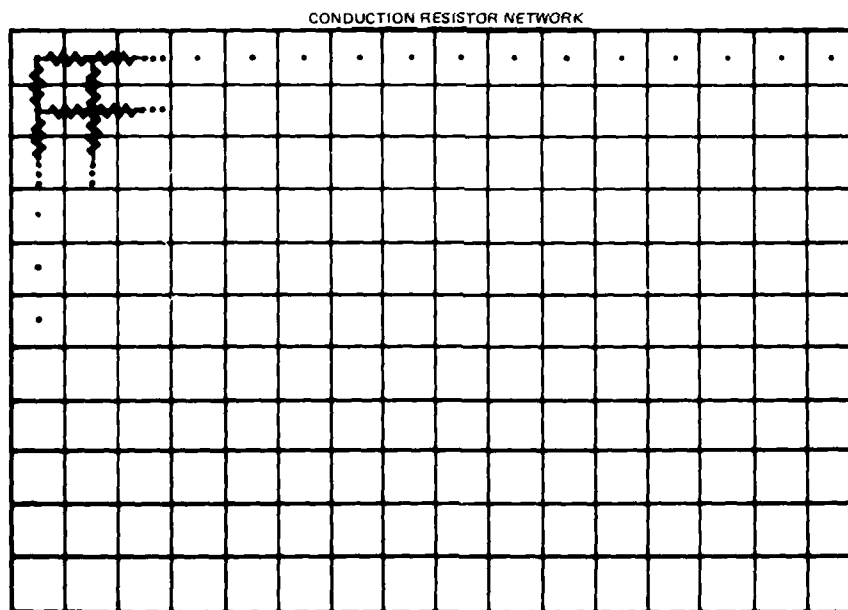


Figure B-2. LMDS module Circuit Board Conduction Resistor Network.

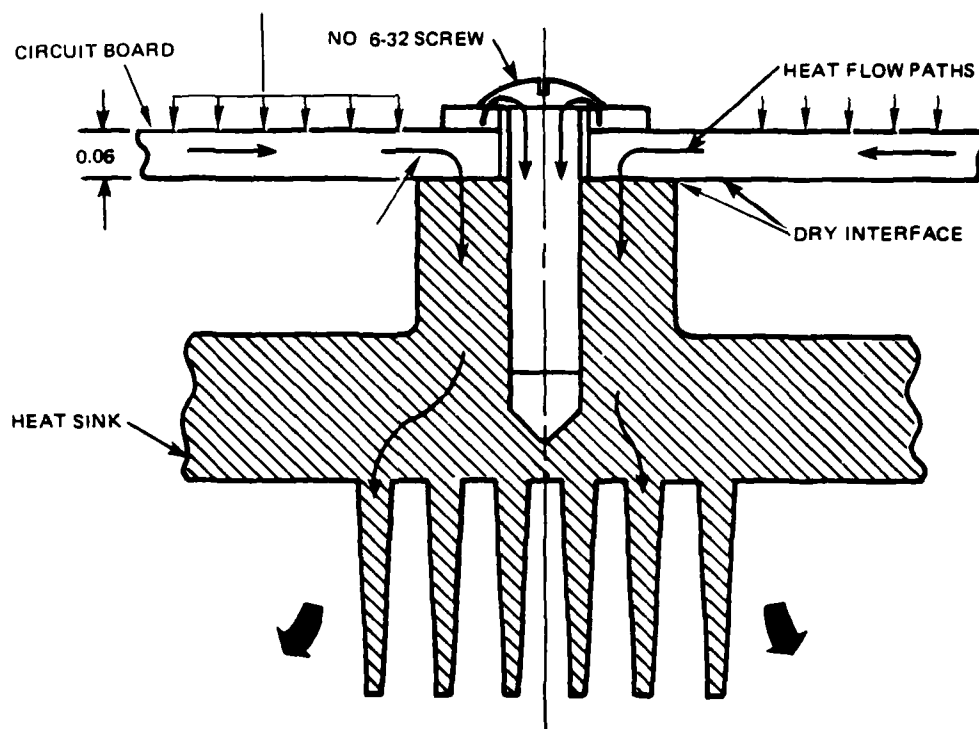


Figure B-3. LMDS thermal model circuit board mounting detail and heat flow paths.

Specific electronic components were undefined and could not be included in the preliminary thermal model. Copper ground planes, power planes, and circuitry were simulated as uniform solid layers across the board by adjusting the thermal conductivity of the board parallel to the surface. The effective conductivity of the circuit board can be calculated by the following equation:

Circuit board effective thermal conductivity =  $K_e$

$$K_e = \frac{K_c t_c + K_B t_B}{t_c + t_B} \quad \text{Eq B-1}$$

where

$K_c$  = copper thermal conductivity

$t_c$  = copper thickness

$K_B$  = epoxy thermal conductivity

$t_B$  = circuit board thickness

The heat sink model was divided into 30 nodal elements interconnected by 48 resistors representing conduction heat flow paths. Nodes that included finned surfaces were connected to ambient temperature air nodes by resistors that simulated natural convection heat transfer.

#### RESULTS OF COMPUTER ANALYSIS

Part Junction Temperatures. The results of the computer analysis are presented in figures B-4 through B-9. The results include the preliminary design maximum allowable temperature limits that have been established based upon reliability and electronic performance requirements. Junction temperatures of typical integrated circuit components expected to be used in the system are plotted in figure B-4 through a range of module total heat dissipations. This was obtained by superimposing the part temperature rise and superimposing this value on the average circuit board temperature predicted by the computer model assuming junction-to-ambient thermal resistance of  $10^\circ\text{C/W}$ . The junction temperature varied from  $60^\circ\text{C}$  to  $88^\circ\text{C}$  for module total heat dissipations of 10 W to 50W, respectively. The preliminary Junction Temperature design limit of  $90^\circ\text{C}$  is exceeded when the module total power dissipation is greater than 42 W. The predicted junction temperature is  $74^\circ\text{C}$  at the design dissipation of 25 W.

Circuit Board Temperatures. The predicted average temperatures of the circuit board and heat sink are plotted in figures B-5 through B-9 for heat dissipation up to 40 W. The average circuit board temperature of both circuit boards was predicted to be  $61^\circ\text{C}$  at the preliminary design dissipation of 12.5 W and well below the maximum allowable part design limit of  $90^\circ\text{C}$  junction temperature. Natural convection or radiation heat transfer from the surface of the circuit board was not considered in the preliminary thermal model. The predicted circuit board average temperature rise above ambient air is presented in figure B-6; it varied from  $5^\circ\text{C}$  to  $28^\circ\text{C}$  for heat dissipations of 5

W and 25 W, respectively. The temperature rise at the design dissipation of 12.5 W is 12°C.

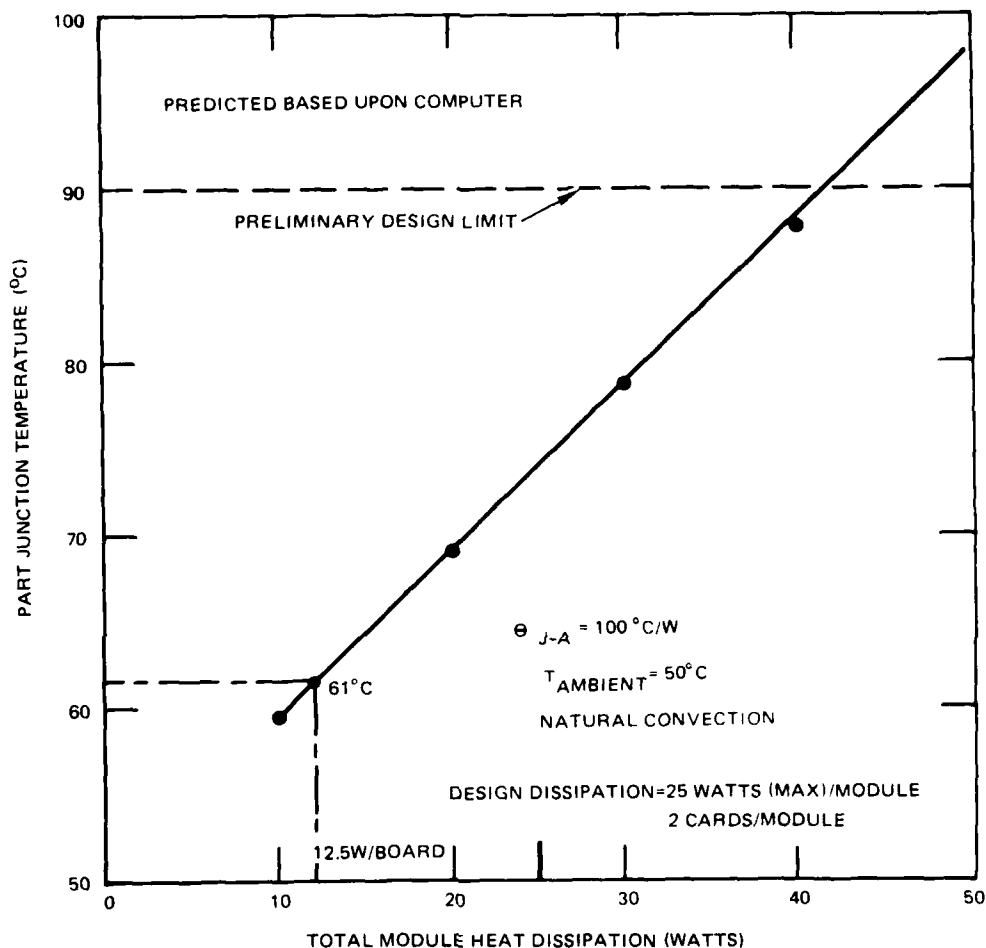


Figure B-4. Predicted integrated circuit junction temperature.

In order to conduct as much heat as possible directly into the heat sink base, the board mounting interfaces must be carefully designed to minimize thermal resistance. The thermal resistance of a particular joint is difficult to predict by analytical techniques, it is usually determined experimentally. Good interface design practice dictates controlling surface finishes -- providing sufficient contact areas, and maintaining adequate contact pressure. Recommended nominal screw joint thermal resistance values for preliminary design analysis were 1.25 hr-°F/BTU for number 6 screws and no interface

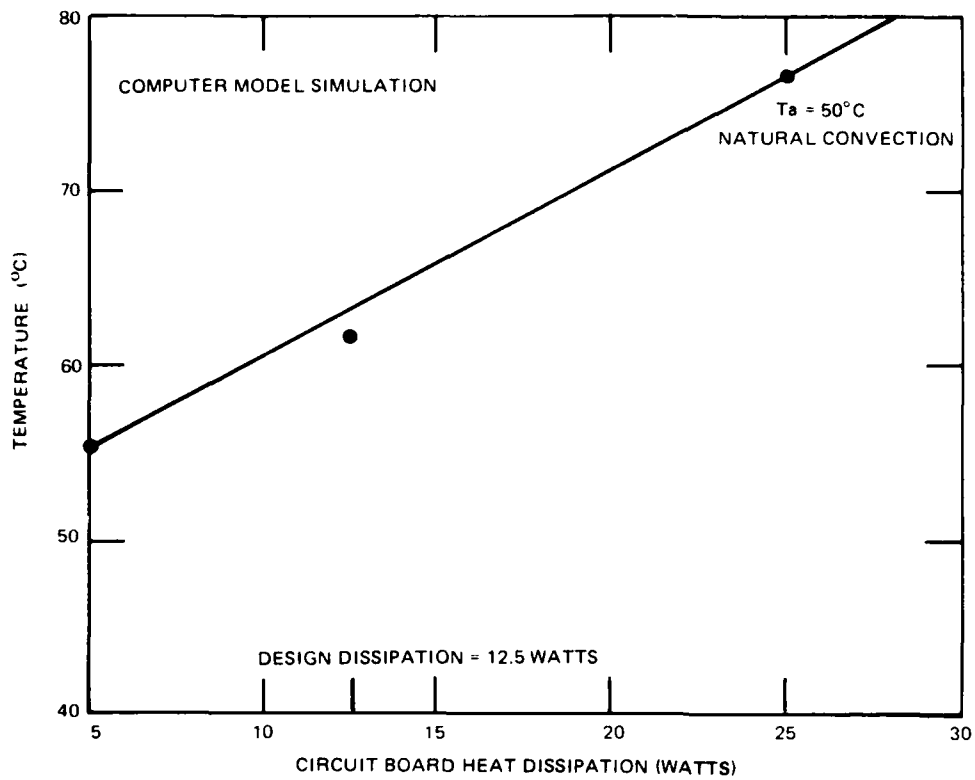


Figure B-5. Predicted circuit board average temperature versus heat dissipation.

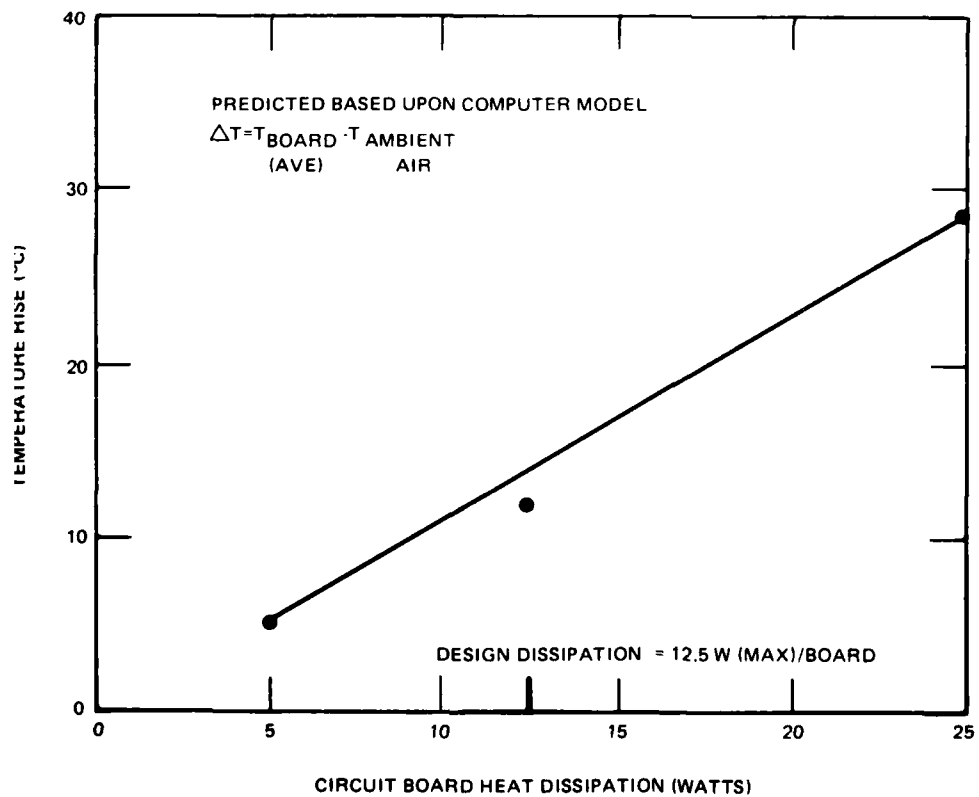


Figure B-6. Predicted circuit board temperature rise versus heat dissipation.

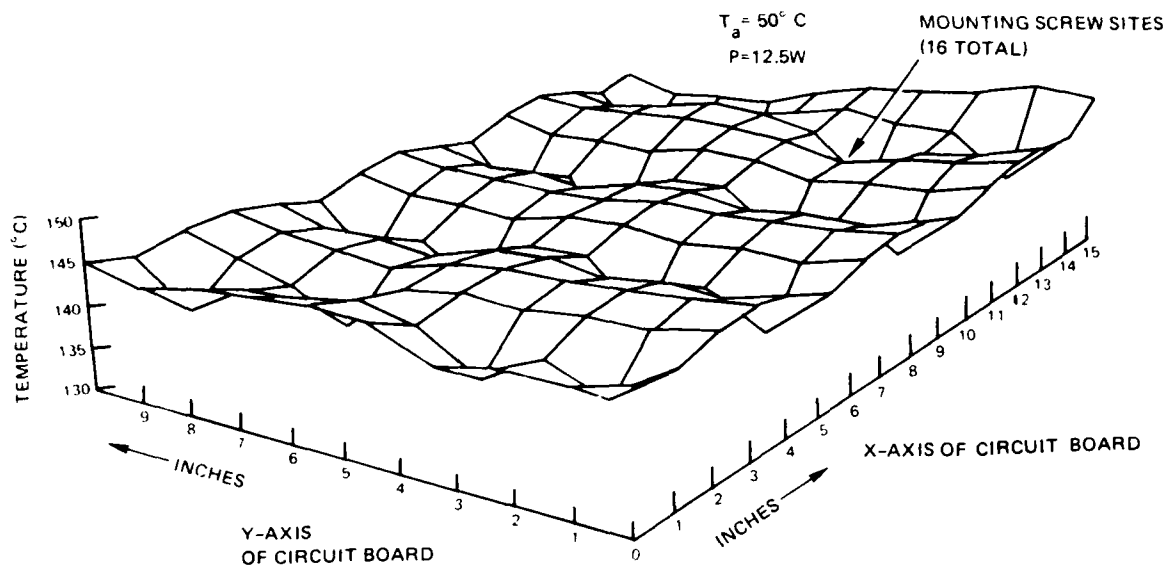


Figure B-7. Thermal gradient plot of predicted circuit board temperature.

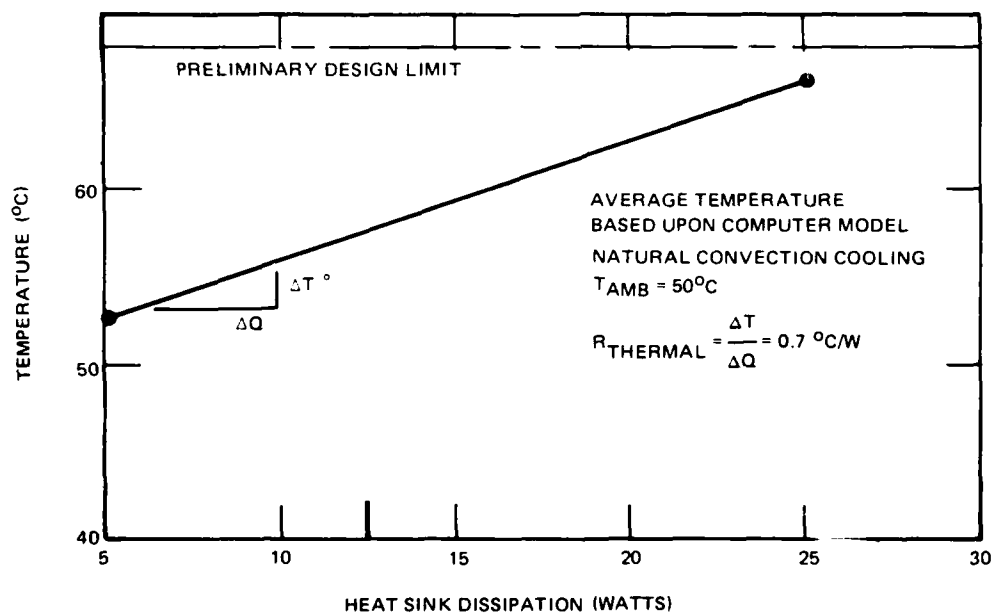


Figure B-8. Predicted average heat sink temperature.

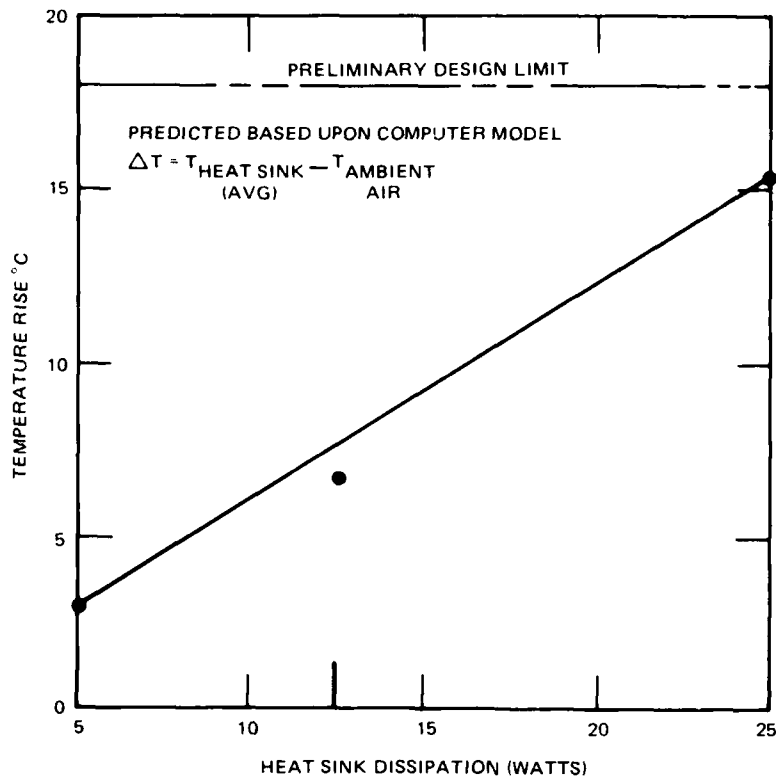


Figure B-9. Predicted heat sink temperature rise.

filler material. A detail of a typical circuit board mounting configuration is shown in figure B-3.

The predicted temperature gradient across the circuit board for a 12.5 W evenly distributed heat load is plotted in figure B-7. Maximum temperature of 65°C occurred near the center and edges of the board. The lowest temperature of 56°C was near the mounting screws. This suggests that parts with high heat dissipations should be located near the mounting screws or be provided with auxiliary methods of coupling heat to the mounting screws.

Heat Sink Temperatures. The predicted average heat sink temperature is presented in figure B-8. The temperature ranged from 52°C to 66°C for 5 W and 25 W. The temperature was 57°C at the circuit board design dissipation of 12.5 W. The maximum temperature gradient across the base was 3°C with 12.5 W



dissipation which indicated good heat spreading with an evenly distributed heat load.

The average heat sink thermal resistance is determined by equation B-2 as follows:

$$R = \frac{T}{Q} = \frac{66-52}{25-5} = 0.7^{\circ}\text{C/W} \quad \text{Eq B-2}$$

The predicted thermal resistance is  $0.70^{\circ}\text{C}$  per watt based on natural convection cooling. The predicted heat sink temperature rise is plotted in figure B-9. A more detailed analysis will be made on high power or temperature sensitive parts when the electrical design is defined.

#### **LMDS MODULE THERMAL TEST SUMMARY**

A thermal test was performed on an electronic module assembly to evaluate the steady-state thermal performance and provide data to evaluate the accuracy of the analytical model. The experimental thermal test module was designed to represent an actual configuration using typical heat sinks, integrated circuit resistors to simulate electronic component heat sources, and a simulated circuit board. The test provided preliminary engineering data to evaluate the circuit board mounting method and establish baseline performance data to compare to new designs. The test was limited to a single module assembly with no adjacent modules or heat sources. No attempt was made to evaluate the transient temperature response of the module or to control the external ambient thermal environment.

#### **TEST OBJECTIVES**

The primary test objectives were to obtain steady-state temperature data, evaluate the module's thermal characteristics and performance, determine internal temperature gradients, and to evaluate the circuit board mounting methods.

## DESCRIPTION OF TEST

The following equipments were used for the tests:

- a. Power supply, Systron-Donner model, 60 V, 20 A.
- b. Temperature recorder, Esterling Angus Speed Servo II, 24 channel multipoint recorder (accuracy =  $\pm 0.25$  percent per span)
- c. Thermocouples, copper-constantan type "T," 30 gauge (accuracy =  $\pm 1$  percent)

Thermocouples were bonded with silver conductive paint and epoxy to ensure good surface contact. The temperature recorder was calibrated by the manufacturer's service representative and the thermocouples were checked in ice and hot water baths prior to testing the module.

The thermal test module was operated through a range of total heat dissipations from 10 watts to 100 watts. The length of each test run was approximately 3 hours or until near steady-state conditions were indicated by negligible temperature changes. The module was located in an area where local air velocities were small to minimize any effects on the natural convection heat transfer.

## DISCUSSION OF RESULTS

The results of the module thermal test are represented in figures B-10 through B-14 with a summary of the temperature data included in table B-1. The junction temperature of the integrated circuit resistors, used to simulate electronic parts mounted on the printed circuit board, is shown in figure B-10 for module total heat dissipations from 10 to 50 W. The part temperature was determined partially by thermal test data, and the following general equations.

$$T_J = T_{AMB} + \overline{T}_{BOARD} + P_D (\theta_{J-A}) \quad \text{Eq B-3}$$

where

$$T_{AMB} = 50^{\circ}\text{C}$$

$$\Delta T_{BOARD} = \bar{T}_{BOARD} \text{ (test average)} - T_{AMB}$$

$$P_D = \text{Part dissipation, W per part}$$

$$\theta_{J-A} = \text{Part thermal resistance junction to ambient} = 96^{\circ}\text{C/W}$$

$$\text{If } P_D = 0.10 \text{ W, } T = 15.5^{\circ}\text{C (test path)}$$

Eq B-4

$$\text{then } T_J = 50 + 15.5 + 0.10(96) = 75^{\circ}\text{C}$$

Eq B-5

This is below the maximum allowable preliminary design limit of  $90^{\circ}\text{C}$  for 25W dissipation. The design limit was exceeded when the total module power dissipation was greater than 40 W.

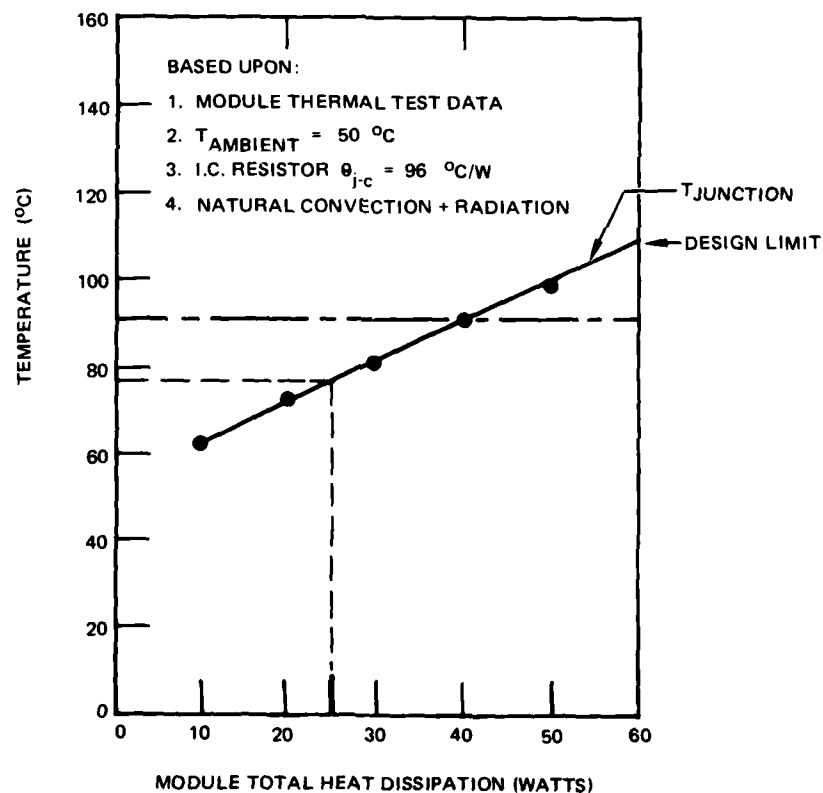


Figure B-10. LMDS module simulated Electronic Part Junction Temperature.

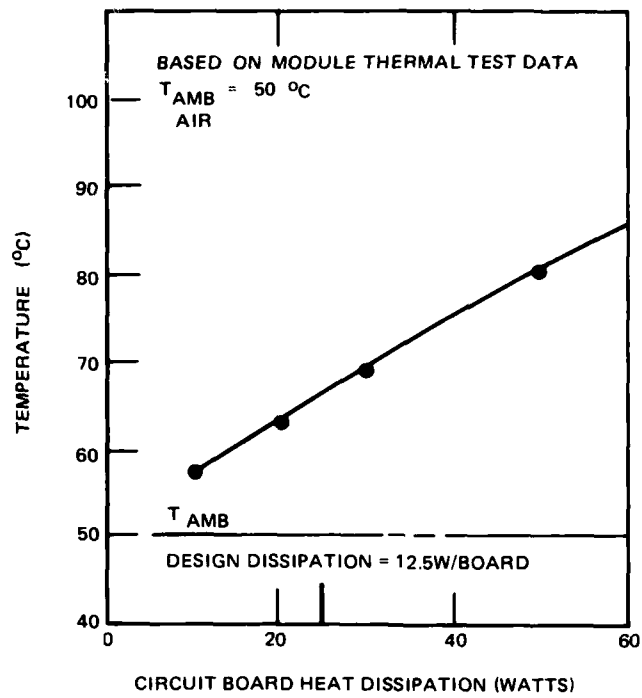


Figure B-11. LMDS circuit board average temperature.

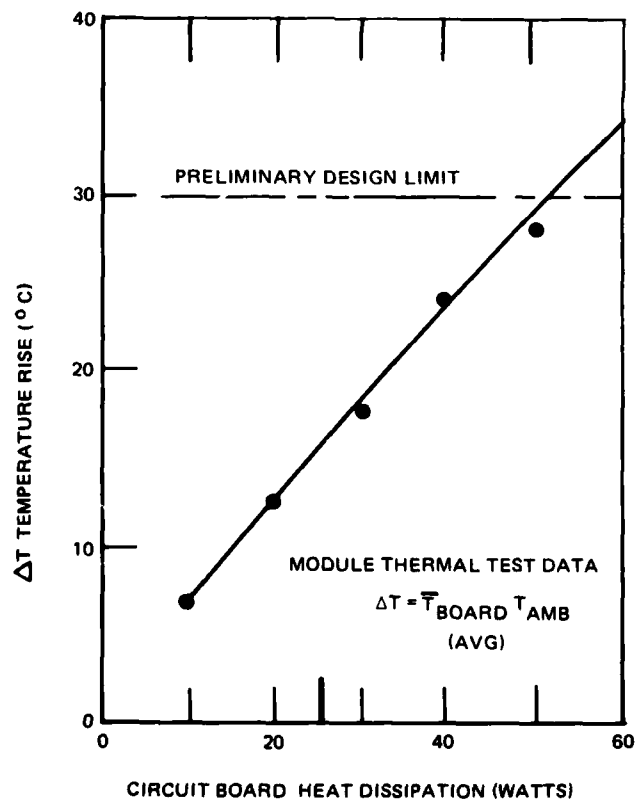


Figure B-12. LMDS module circuit board temperature rise.

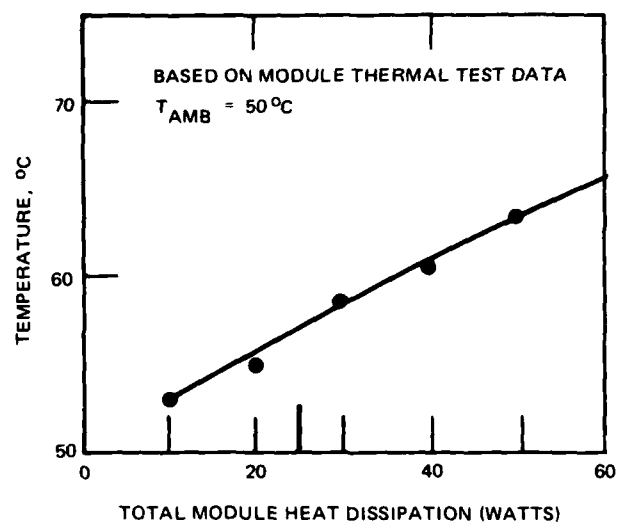


Figure B-13. LMDS module heat sink temperature.

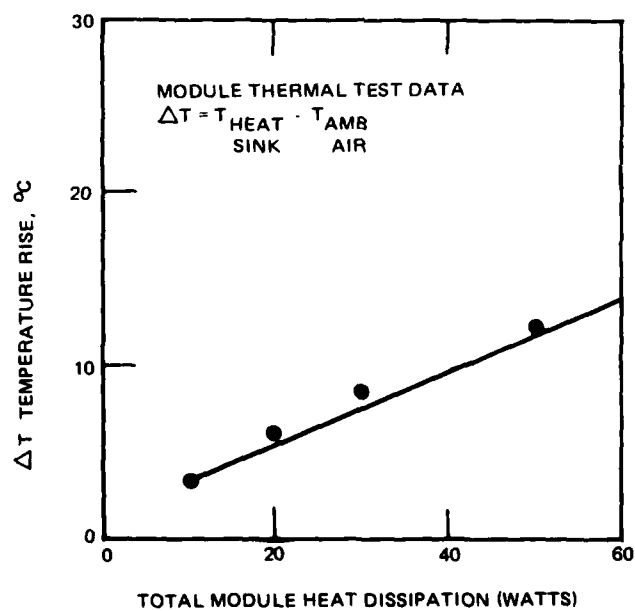


Figure B-14. LMDS head sink base temperature rise.

Table B-1. Module test circuit board mounting interface data summary.

$Q$ Dissipation, Total Module	Watts Per Screw	T15 °F	T6 °F	$\Delta T = T_{15}-T_6$ °F	$R = \frac{\Delta T}{Q}$ °F/W	T7 °F	$T = T_6 T_7$ °F	$R = 6-7$ °F/W	$\Sigma R$ °F/W
10	0.31	88	83	5	16.1	81	2	6.45	22.5
20	0.62	97.5	87.5	10	16.1	84	3.5	5.64	21.7
30	0.94	109	95	14	14.8	90	5	5.32	20.1
40	1.25	122	102.5	20.5	16.4	44	8.5	6.8	23.2
50	1.56	132.5	108	24.5	15.7	100	8.0	5.1	20.8
								$\bar{R} =$	21.8

The circuit board average temperature and temperature rise is shown in figures B-11 and B-12. The test data have been adjusted to an ambient temperature of 50°C to illustrate anticipated worst case operating conditions. The average board temperature and temperature rise at a power dissipation of 12 1/2 W was 66°C and 16°C, respectively.

The module heat sink average base temperature and temperature increase is plotted in figures B-13 and B-14 through a range of heat dissipations. The base temperature varied from 53°C to 63°C for module total heat dissipations from 10 W to 50 W, respectively, at an adjusted ambient air temperature of 50°C. The heat sink base average temperature rise above ambient varied from 3°C to 14°C through a range of 10 W to 50 W dissipation. The temperature rise was 8°C at the module design dissipation of 25 W.

#### CIRCUIT BOARD MOUNTING INTERFACE THERMAL RESISTANCE

The temperature gradient across a typical circuit board mounting screw joint was measured in order to estimate the overall interface thermal resistance. An accurate determination of the interface resistance cannot be made because heat flow rates through the individual joints are unknown. However, assuming the heat dissipated by the integrated circuits is distributed uniformly across the board and conducted through the mounting screws interface thermal resistance may be estimated. A typical thermocouple location and mounting detail is shown in figure B-15 for the prototype construction to be employed. A summary of the interface temperature gradient and calculated thermal resistance is shown in table B-2 for a range of heat dissipations. The estimated overall interface thermal resistance per screw is 12° C/W assuming the total heat dissipation is conducted through the screw joints. An expected range would be from 10° C/W to 20° C/W (per mounting screw interface) assuming only a portion of the heat is transferred directly to the heat sink by conduction through the joints. This value is much higher than preliminary design nominal value of 2.6° C/W per mounting point based upon the screw size.

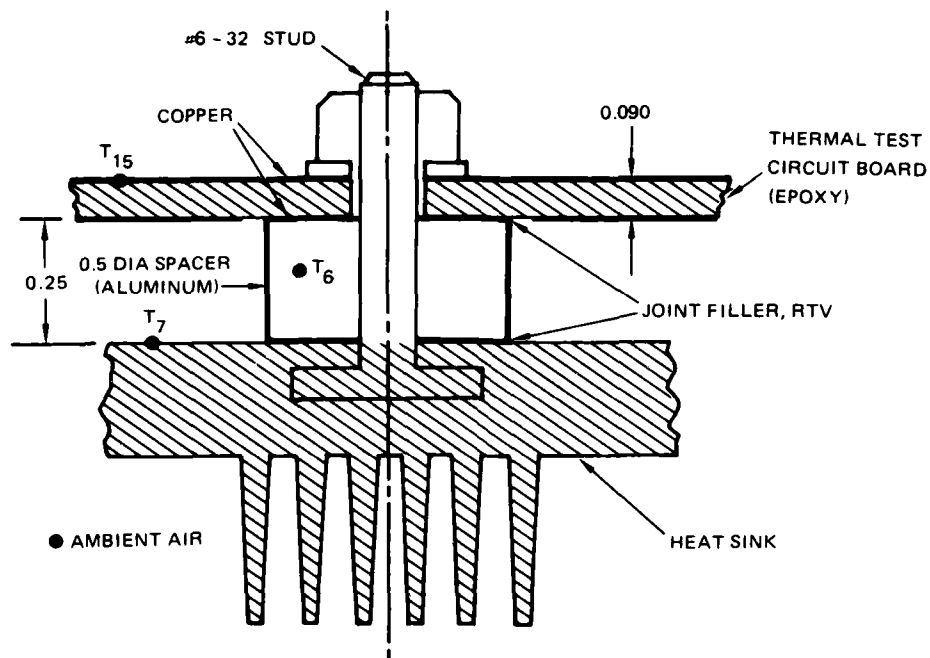


Figure B-15. Circuit board mounting thermocouple locations.

This discrepancy is partially due to the circuit board material thickness being included in the module thermal test configuration and was not considered in the computer thermal model. Design modifications will be investigated to reduce the interface thermal resistance and temperature gradient across the mounting points.

A comparison of the circuit board and heat sink temperatures predicted by the computer model and the test results are plotted in figures B-16 and 17. The data indicate that a reasonable correlation was obtained between the experimental and analytical results.



Table B-2. Circuit Board Mounting Temperature Data.

Q WATTS/MODULE	TEMP, °F			$\Delta T$ ( $T_{15} - T_7$ )		$R = \Delta T / P_D$ °C/W
	$T_{15}$	$T_6$	$T_7$	°F	°C	
10	88	83	81	7	4	12.9
20	98	88	84	14	8	12.9
30	109	95	90	19	11	11.7
40	122	103	94	28	16	12.8
50	133	108	100	33	18	11.5
						<hr/> ΣR = 12.3
$P_D = Q / \text{SCREWS} = \text{WATTS/SCREW}$						

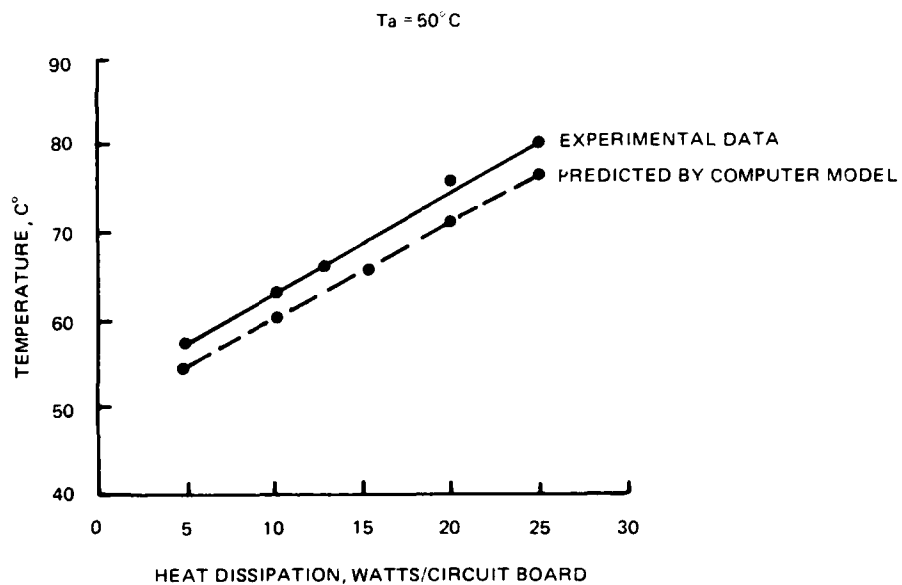


Figure B-16. Comparison of predicted average board temperature and test results.

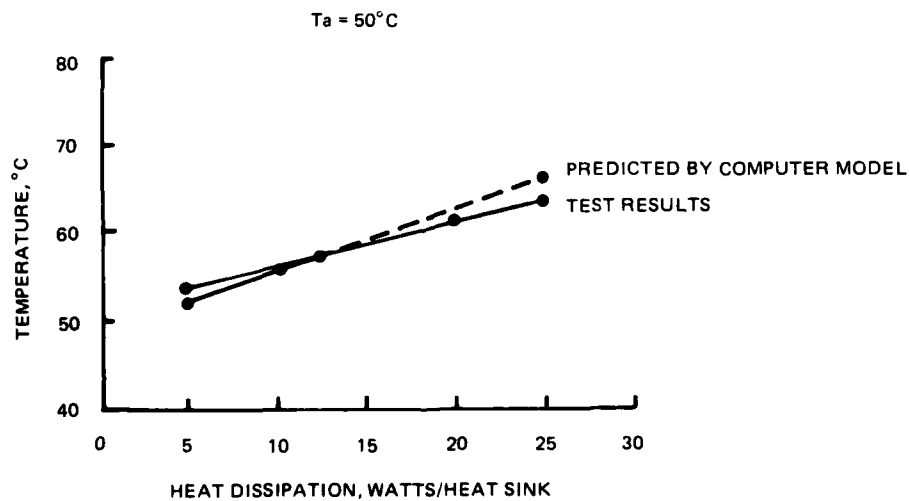


Figure B-17. Comparison of predicted average heat sink temperature and test results.

APPENDIX C  
LMDS SHOCK AND VIBRATION TEST DATA

INTRODUCTION

A Lightweight Modular Display System (LMDS) framework was designed to meet the shipboard vibration requirements of MIL-STD-167-1 and high impact shock requirements of MIL-S-901C. Before structural material was procured and assembled, an analytical model was created using the NASA Structural Analysis Program (NASTRAN). NASTRAN is a finite element program capable of static and dynamic analysis of large structural systems. Several structural iterations were made before the design was acceptable. The following discussion includes a description of the structural model, the applied forces, and analytical results. Also included is the exploratory vibration test setup and test results of the fabricated framework.

ANALYTICAL DISCUSSION

ANALYTICAL TECHNIQUES

NASTRAN is a general purpose digital computer program designed to analyze the behavior of elastic structures under a range of assumed loading conditions using a finite-element displacement method. The displacement of each element is found by applying basic stress and strain equations. The program is applicable to most linear and some nonlinear structures that can be represented by combinations of finite elements such as rods, bars, plates, and concentrated masses, each of which is provided with sectional properties, material properties, and mass properties. These elements are placed into a coordinate grid system where identifiable points of the elements (called grid points) are referenced with respect to the coordinate system. The elements are then formed into a mass matrix and a stiffness matrix using the element properties and geometry. It is also possible to introduce structural and viscous damping to form a damping matrix; damping is not included in this analysis. In order to stress the structure, a force matrix must be introduced. The forces in this analysis include model gravitational forces and shock table inertial forces.

Based on the foregoing information, the following matrix equation can be written:

$$[M] \ddot{X} + [K] X = [F(T)]$$

where  $[M]$  is the mass matrix  
 $\ddot{X}$  is the acceleration matrix  
 $X$  is the displacement matrix  
 $[K]$  is the stiffness matrix  
 $[F(T)]$  is the forcing function matrix

Two analyses were performed on the LMDS structure. The first was a modal modes (vibration) analysis. From the previous equation, the structural normal modes (natural frequencies) can be found:

$$[W^2] = [M^{-1}] [K]$$

where  $[W^2]$  is the natural frequency matrix.

There is one natural frequency for each degree of freedom in the model. The important natural frequencies are side-to-side, fore-to-aft, and vertical. These have most of the structural masses moving in the same direction in phase.

The second analysis of the LMDS structure was a modal transient (shock) analysis. This method solves for the response of a structure to time-varying loads. The differential equations of motion are reformulated in terms of modal coordinates in an uncoupled set. Integration is performed by finite differences on the uncoupled modal differential equations. This yields the time-varying displacements, velocities, accelerations, and constraint forces at grid points and the time-varying forces and stresses in elements. This method was used to model the LMDS structure on the shock table to meet the requirements of MIL-S-901C.

## STRUCTURAL MODEL

The LMDS structure was modeled from NOSC drawing 105464. There were several iterations made before the structure members were sized. Rather than simulate the vibration test of MIL-STD-167-1, the structure was designed to eliminate all natural frequencies below 50 Hz. The frequency of 50 Hz was picked rather than 33 Hz or some other lower frequency because of the trend to new higher speed ships. The structure was also designed to carry the shock loads from MIL-S-901C. The structure was made with 6061-T6 aluminum alloy which has a yield strength of 40 000 psi. A safety factor of 2.5 was used to account for welds and modeling inaccuracies. The welding reduces the 6061-T6 to an untempered condition in the area of the joints. The design stress limit was set at 16 000 psi.

The structural model is shown in figure C-1. It is 21.5 inches wide, 18 inches deep, and 45 inches high. The structure is composed of three levels. The first level has three 25-pound modules that are 5 by 11.5 by 16.5 inches. The second level has three more 25-pound modules. The third level is composed of a "bull-nose" keyboard area weighing 8 pounds and is at a convenient height for a seated operator; it has a 55-pound CRT alongside a seventh 25-pound module. These three levels are maintained by the support structures composed of a 1-1/4-inch by 1-1/4-inch by 1/8-inch square tube, a 1-inch by 1-inch by 1/8-inch square tube, a 3/4-inch by 3/4-inch by 1/8-inch square tube, a 1-1/4-inch by 1-1/4-inch by 1/8-inch angle, and four thicknesses of plates of 1/4, 3/16, 3/32, and 1/16 inches. The seven modules and CRT were not modeled in detail but were simulated by distributing 1/8 of the weight at each of the attachment points. The grid points were numbered 1 through 56. The support structure was modeled by 67 bar elements, 19 quadrilateral elements, and 6 triangular elements.

As with any analytical model, there were simplifications. The real structure has an unlimited number of degrees of freedom, whereas the number of degrees of freedom in the model was equal to the number of grid points times six minus the number of single point constraints. Another simplification was that in the real structure, the joints were welded (fixed), bolted, riveted, and pinned and, in the model, the joints were all fixed (welded).

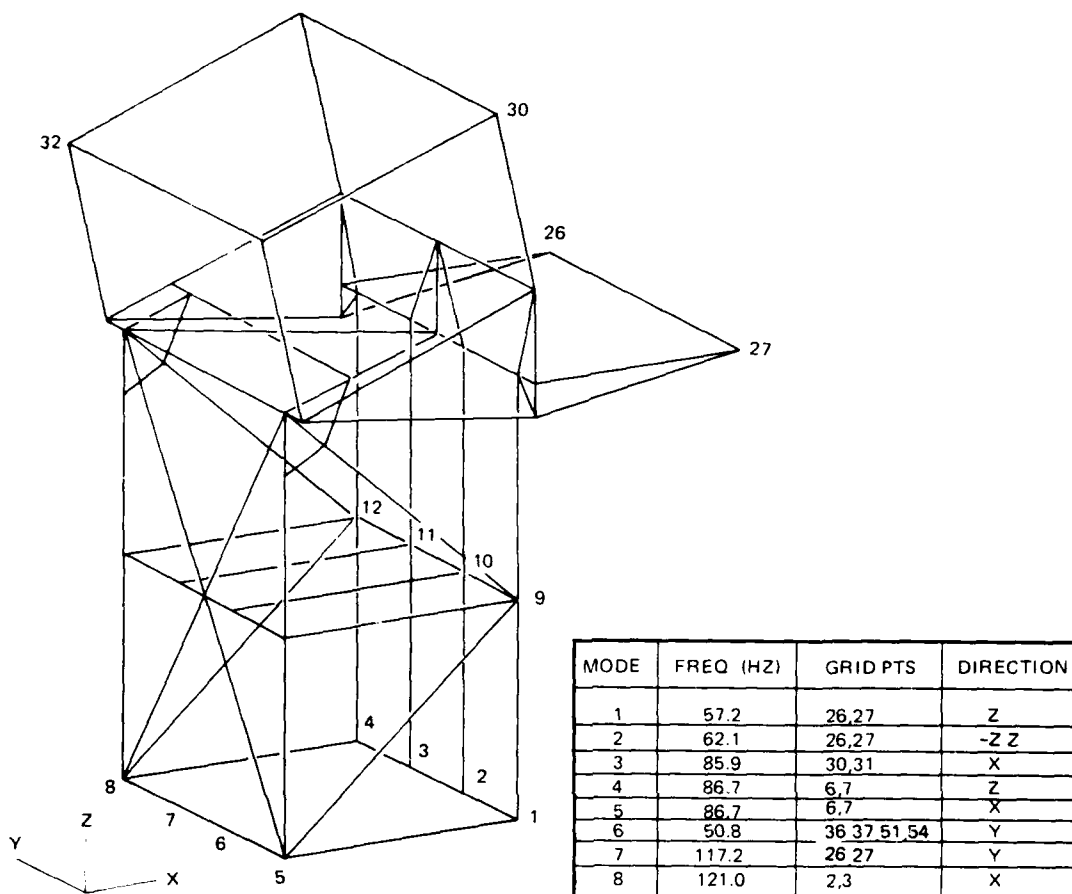


Figure C-1. Display console structural model.

This made the structure appear to have slightly higher natural frequencies than with joints that were less fixed. There were two areas of bolted joints in the real structure that were considered welded in the model. The first area was at the top of the four legs where the CRT and bull-nose framework was interfaced. The framework was fastened to the leg tops with four expandable bolts. The second area was at the interface of the structure and the deck. In the model, the structure was considered welded to the deck at the base of the four legs. The real structure was bolted to the deck with four bolts. A third simplification was that all internal components (modules, CRT, cabling, etc) were distributed as concentrated weights at nearby grid points in a way that preserved the overall weight, center of gravity, and moments of inertia.

## EXTERNAL LOADS

The shock analysis required an external forcing function to determine the structure's response to the shock table. The forcing function (or shock load) shown in figure C-2 was obtained from the medium weight shock machine. This forcing function was applied to the structure when tilted at 30° backwards and 30° sideways as shown in MIL-S-901C.

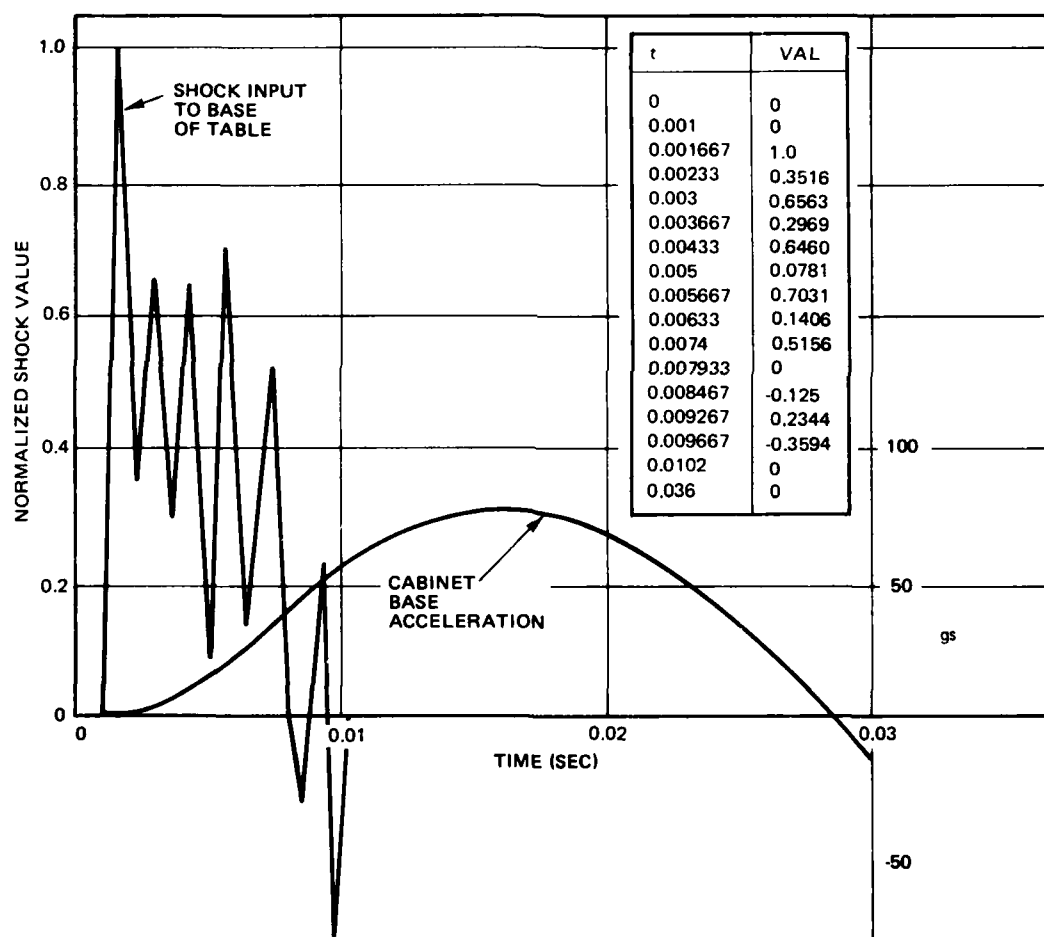


Figure C-2. Tilted shock load.

## ANALYTICAL RESULTS

The natural frequency results are shown in figure C-1. The first natural frequency was at the bull-nose (or tablet shelf). It vibrated vertically as a cantilever at 57 Hz. The second natural frequency was the shelf end points vibrating out of phase in the vertical direction at 62 Hz. The third natural frequency was the fore-to-aft vibration of the structure at 86 Hz. This was considered to be the fundamental frequency at which the structure vibrated as a body in one direction. The fourth and fifth natural frequencies were the two side-to-side vibrations of the bar element connecting grid points 5 and 8. The sixth natural frequency was considered to be the second fundamental frequency of the LMDS structures. The structure model vibrated in the side-to-side (Y) direction at 91 Hz. All other vibration modes were above 100 Hz.

There was no attempt to simulate the test given in MIL-STD-167-1 for vibration. Since the standard calls out vibration only for 4 to 50 Hz, the reasoning was that if all natural frequencies were above 50 Hz there would be no resonance problems.

The simulated shock test analytical results are shown in figures C-3 and C-4. The shock load was applied at the bottom of the four vertical members. These members model the 30° shock mount as shown in MIL-S-901C. The most highly stressed area for the 30° backward tilt model was at the framework interface just below the CRT and top module. The maximum combined (bending, torsional, and axial) stress was 12 681 psi compression. The maximum combined bending stress in the legs was 10 220 psi compression. Both of these stresses were well below the aluminum 6061-T6 yield stress of 16 000 psi. The most highly stressed area for the 30° side tilt model was at the bottom of the bar member 51. The stress in this area was 16 263 psi tension which was right at the yield stress. Leg bar members 9 and 12 and diagonal member 53 were also highly stressed but below the yield limit. To correct the condition in member 51 a second tube 1 inch x 1 inch x 1/8 inch square was nested inside the 1 1/4 inch square tubing to share the load and maintain the design safety factor.



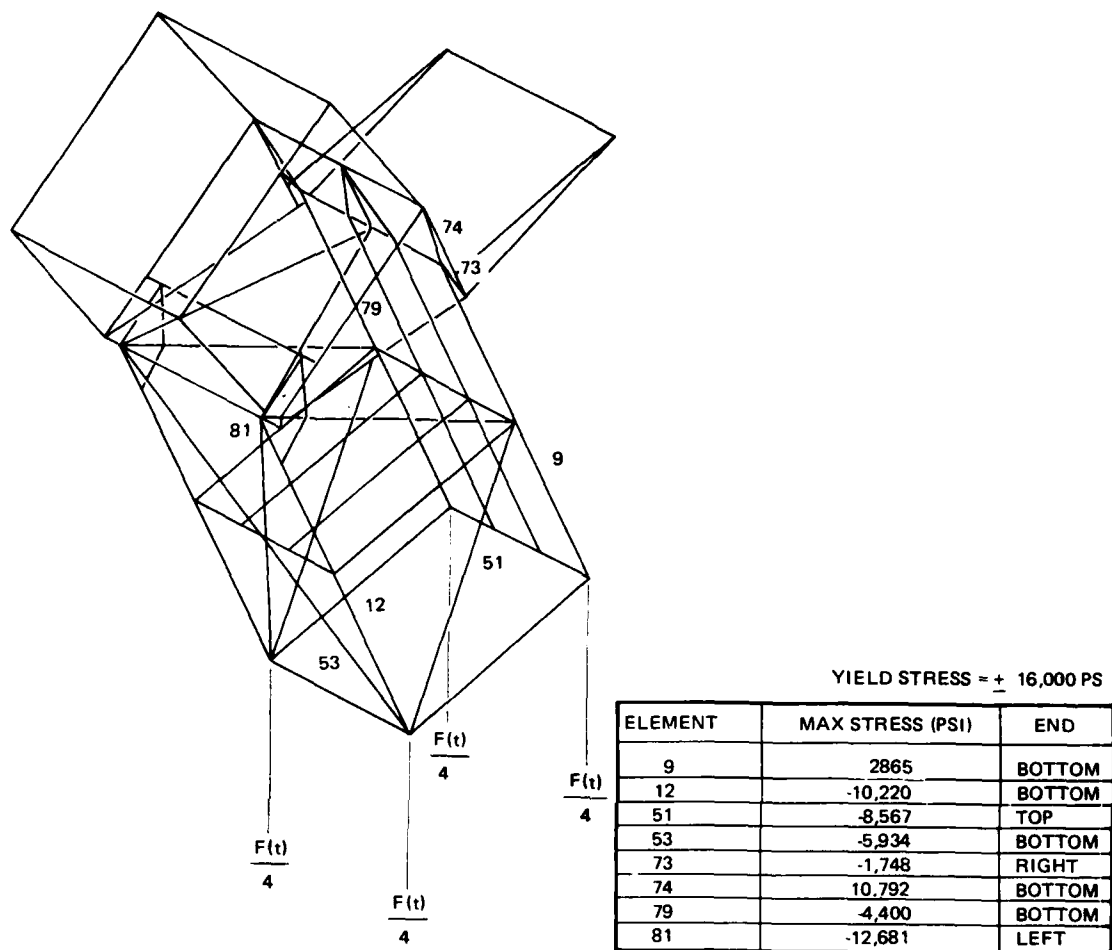


Figure C-3. Display console backward tilt shock model.

## VIBRATION TEST DISCUSSION

### PURPOSE OF TEST

The purpose of the test was to collate the analytical results with a low level vibration response of the weighted structure. The exploratory vibration ranged in frequency from 5 Hz to 22 Hz, maintaining a constant double displacement of 0.02 inch, and from 22 Hz to 100 Hz maintaining a 0.5 g constant acceleration.

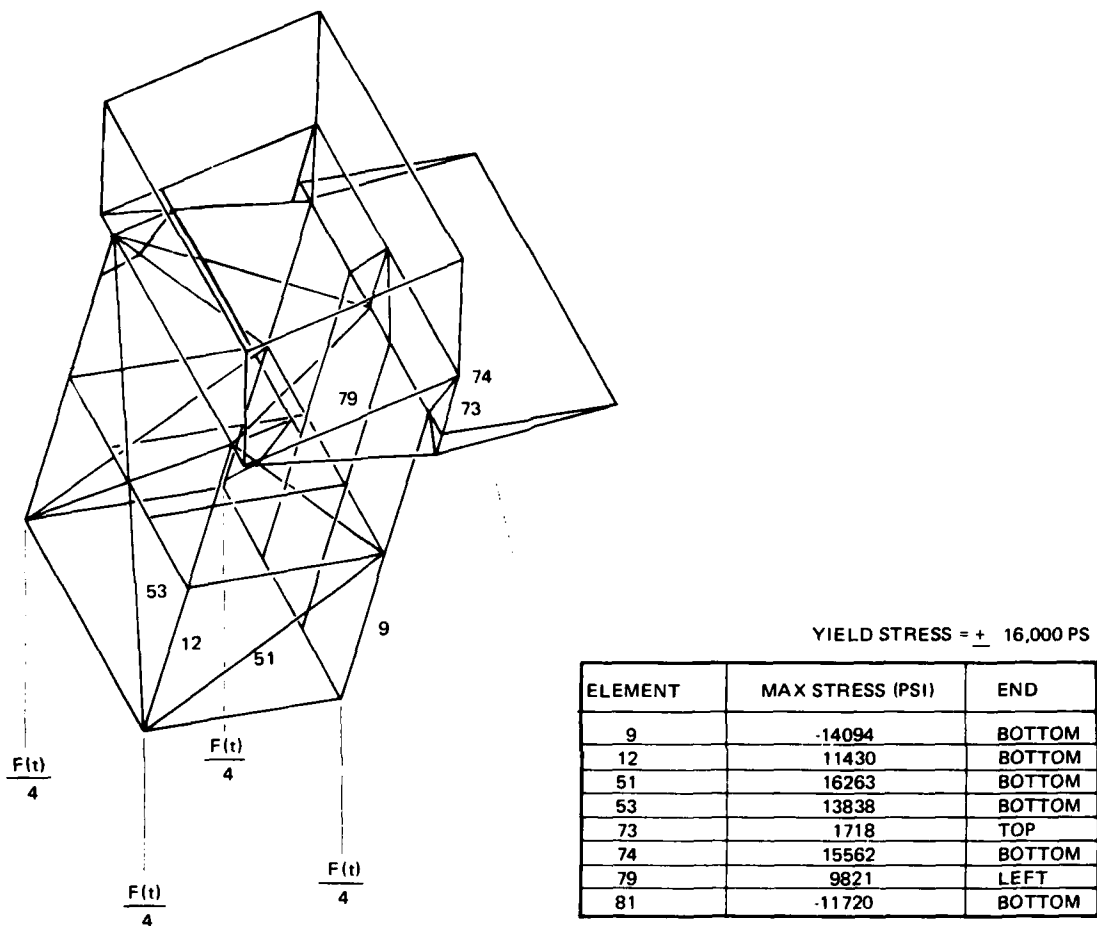


Figure C-4. Display console side tilt shock model.

#### TEST SET-UP

The analytical frame was fabricated and the electronic modules were installed. Dummy loads were secured to the modules, CRT frame, and bull-nose to provide the loading used in the computer analysis. Each module with dummy loading weighed 25 pounds. The CRT was ballasted with 32 pounds to make a total CRT weight of 55 pounds. Eight pounds of weight were added to the bull-nose. Total weight was 275 pounds.

The base of the structural frame was secured to the vibration table (Calioyne Model 177) with six steel bridge clamps. Thirteen accelerometers were mounted on the test structure. The tests were conducted in three orthogonal axes, front-to-back (X), side-to-side (Y), and vertical (Z).

A schematic of the test setup is shown in figure C-5. The test structure was mounted on a Calioyne Model 177 exciter. A control accelerometer was mounted on the vibration table. The output from this accelerometer was received by a signal conditioning amplifier (MB N400) and passed on to a sweep oscillator and power amplifier. The exciter was controlled by the

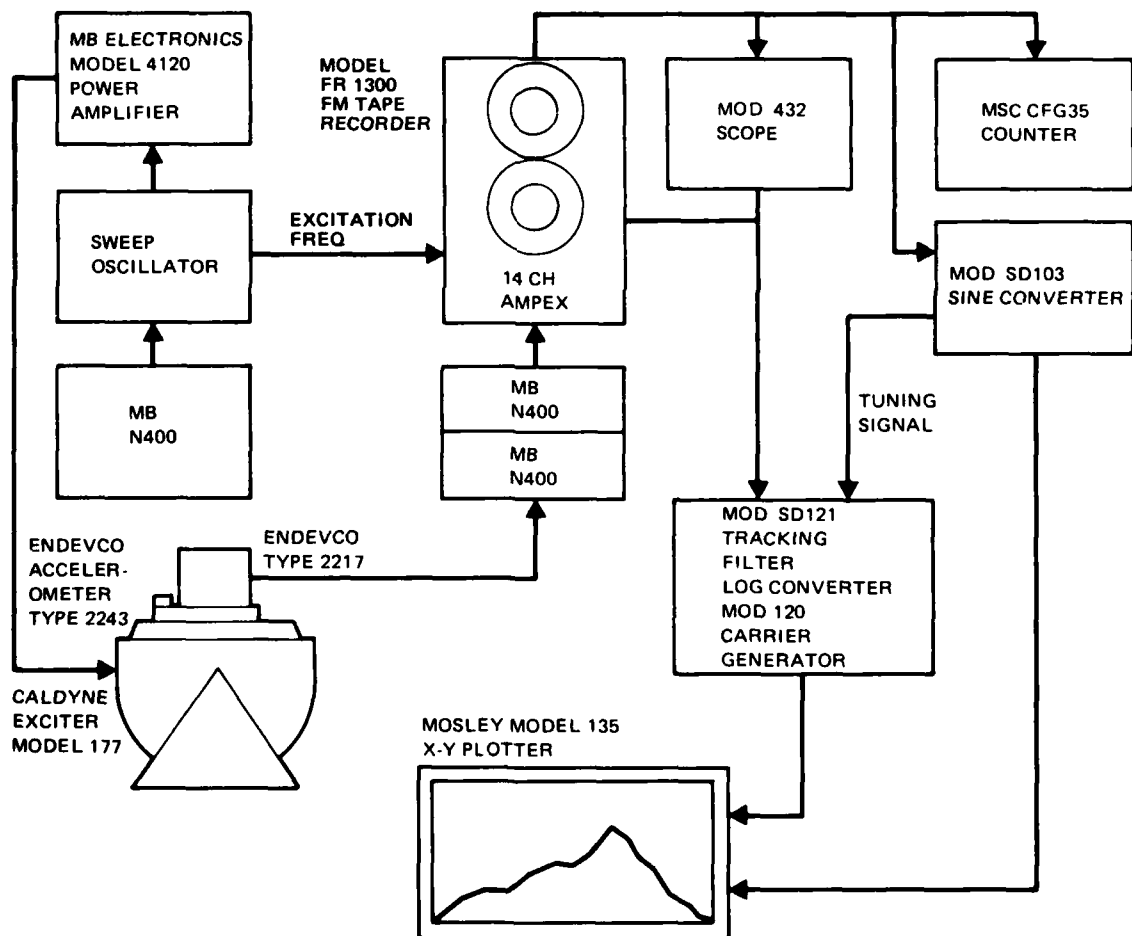


Figure C-5. LMDS vibration test instrumentation diagram.

sweep oscillator and power amplifier, with feedback from the control accelerometer. The sweep oscillator was programmed to advance 3 Hz per minute. The other 12 accelerometers were mounted on various points of the structure with the output received by a signal conditioning amplifier (MB 400) and recorded on a tape recorder. Later, the signal on each channel was passed through a sine converter, tracking filter, log converter, and carrier generator, with the resulting response plotted on a Mosley X-Y plotter.

#### VIBRATION TEST RESULTS

Three sweeps from 5 to 100 Hz were made for each of the three orthogonal axes. Tables C-1, C-2, and C-3 highlight these results. The resonance frequency and transmissibility results for the front-to-back axis are shown in table C-1. The main structural resonance front-to-back was at 30 Hz. This yielded a transmissibility of 3.8 at the front of the shelf, 3.2 at the top of the legs, and 5.4 at the top of the CRT. The second resonance was at 44 Hz with a transmissibility of 4.3 at the top of the CRT. A third resonance was recorded at 72 Hz.

The resonance frequency and transmissibility results for the side-to-side axis are shown in table C-2. The main structural resonance side-to-side was also at 30 Hz. This yielded a transmissibility of 3 to 4 at the middle of the structure and 5.8 at the top. The second resonance was at 45 Hz with a maximum transmissibility of 7.2 at the top of the CRT. A third resonance was recorded at 88 Hz.

Table C-1. Front-to-back X-axis LMDS  
exploratory vibration test.

Accel No	Axis	Freq (Hz)	TR	Freq (Hz)	TR	Freq (Hz)	TR	Freq (Hz)	Tr
2	Y	5-100	1:1						
3	X	30	2.2:1			70	1.3:1		
4	Y	5-100	1:1						
5	Z	30	4:1			73	5.6:1	100	14:1
6	Z	30	3.8:1			78	3.4:1	100	16:1
7	Y	5-100	1:1						
8	Z			42	2:1				
9	X	30	3.2:1	42	1.6:1			94	2:1
10	Y	5-100	1:1						
11	Z	30	2.2:1			72	1.6:1	100	1.4:1
12	X	30	5.4:1	44	4.3:1	71	7:1		
13	Y			42	1.2:1	72	2.6:1		

Table C-2. Side-to-side Y-axis LMDS  
exploratory vibration test.

Accel No	Axis	Freq (Hz)	TR	Freq (Hz)	TR	Freq (Hz)	Tr	Freq (Hz)	TR
2	Y	5-100	1:1						
3	X	5-100	1:1						
4	Y	30	3:1	46	2.6:1	88	2.8:1		
5	7	34	3:1			76	3.4:1	100	6:1
6	7	30	4:1	44	2.4:1	88	12:1		
7	Y	30	3.6:1	44	2:1	88	2.4:1		
8	7	30	1.4:1	36	1.9:1				
9	X					90	1.6:1	96	1.8:1
10	Y	30	3:1	45	3.4:1				
11	7	30	1.6:1	45	1.6:1	88	2.6:1		
12	X	34	3.4:1	45	1.6:1	66	6:1		
13	Y	30	5.8:1	45	7.2:1	87	2.4:1		

The resonance frequency and transmissibility results for the vertical axis are shown in table C-3. The first vertical structural resonance was at 68 Hz at a transmissibility of 2.4. There was also a cross-coupling resonance in the X direction at the top of the CRT with a transmissibility of 10. Second and third resonances occurred at 84 and 95 Hz.

Table C-3. Vertical Z-axis LMDS  
exploratory vibration test.

Accel No.	Axis	Freq (Hz)	TR	Freq (Hz)	TR	Freq (Hz)	TR
2	Y					94	2:1
3	X	42	1.5:1	70	2.6:1	94	1.8:1
4	Y			84	1.9:1		
5	Z	64	2.4:1			95	14.:1
6	Z	68	2.8:1	84	9.6:1	96	16.4:1
7	Y			84	1.4:1	100	4:1
8	Z			83	2:1	100	2:1
9	X	70	2.4:1	82	1.4:1	100	1.6:1
10	Y	70	1.3:1	82	1.2:1		
11	Z	68	2.4:1	82	4:1	95	5.4:1
12	X	70	10:1			95	5.6:1
13	Y			84	4.8:1		

#### COMPARISON OF ANALYTICAL AND TEST RESULTS

Table C-4 compares the fundamental frequencies for the analytical and test results.

Table C-4. Fundamental frequencies.

	Analytical Frequencies (Hz)	Test Frequencies (Hz)
Fore-to-aft	86	30
Side-to-side	91	45
Vertical	100	68

Clearly, the results do not compare very well. After comparing the analytical model with what was tested, some obvious differences were noted. The first difference was in the way the structure was fastened to the deck. In the analytical model, the structure was assumed to be welded to the deck. In the actual tests, the structure was clamped to the vibration table with three clamps along each of the 1-1/4 by 1-1/4 by 1/4-inch equal leg angles. There was one clamp at the middle of each angle and one 2 inches from each end. The two angles and twelve 3/8 by 1-3/4-inch steel bolts had much more flexibility than if the four legs were welded to the table. The analytical model was changed to simulate the clamping. The results are shown in table C-5.

Table C-5. Fundamental frequencies.

	Clamped Base Analytical Frequencies (Hz)	Test Frequencies (Hz)
Fore-to-aft	30	30
Side-to-side	44	45
Vertical	77	78

It is obvious from the results shown in table C-5 that the method of fastening the structure base to the deck makes a large difference in the fundamental modes of vibration. The best method of attachment would be to weld the structure to the deck. Next best would be to weld the base to a thick plate and bolt the plate to the deck. A third option would be to weld a special corner block to each leg that could be bolted to the floor. The latter approach has been adopted.

Another difference between the analytical model and tested structure was in the way the dummy load was attached to the CRT. In the analytical model the load was distributed among the CRT grid points. In the tested structure, an 8-pound steel plate was bolted with four 1/4-inch steel bolts to an 8-pound aluminum plate. Two of these were made, with one bolted to the rear of the CRT and one bolted at the front. All of these bolts acted like stiff springs with the attached masses able to move in all three directions when under vibration. Accelerometers 11, 12, and 13 were glued to this spring-mass system.

A third noticeable difference was in the first natural frequency of the shelf. The analytical model showed a resonance at 57 Hz. The real structure showed a shelf resonance at 95 Hz. The difference can be accounted for in the way the shelf structure was welded together. The structural triangle on each side of the shelf turned out to be somewhat smaller than the analytical model due to the cross-sectional size of the square tube. This means the frequency will be somewhat higher.

#### **FUTURE TEST REQUIREMENTS**

Future test requirements will include vibrating the structure to MIL-STD-167-1 and shocking to MIL-S-901C. The base mounting has been redesigned to more firmly attach the four legs to the deck or test-bed in preparation for these tests.

Future testing will be delayed until more accurate weights and the actual electronic hardware have been installed. This will make the tests more valid and should increase the fundamental frequencies since the actual weights are expected to be less than the dummy weights.



**DATE**  
**ILME**